Parameter Estimation of Expectation Maximization Algorithm for Intensity Inhomogeneity Correction in Brain MR Images

M.Tech. Dissertation Report

A dissertation submitted in partial fulfillment of the requirement for the M. Tech.(Computer Science) degree of the Indian Statistical Institute

By

Shashank Singh

CS0721

Under the guidance of

Dr. Pradipta Maji

Assistant Professor

Machine Intelligence Unit

Indian Statistical Institute, Kolkata

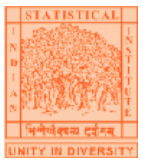

INDIAN STATISTICAL INSTITUTE

203,Barrackpore Trunk Road

Kolkata 700108

Acknowledgments

With great pleasure and sense of obligation I express my heartfelt gratitude to my guide **Dr. P Maji**(Machine Intelligence Unit) . I am highly indebted to him for his invaluable guidance and his readiness for anytime help. His persisting encouragement, everlasting patience and excellent expertise in subject have benefited to an extent, which is beyond expression.

I want to express my sincere thanks to the website **Brain-Web** $(http://www.bic.mni.mcgill.ca/brainweb/selection\_normal.html)$ for providing the synthesized brain MRI s , without which , my project could not be successful.

I also want to thank to Manoj Kumar Nanda (MTech, ISI Kolkata) for his motivation and encouragement and Ashish Singh(MTech, ISI Kolkata) for his noble and helpful nature.

Without wasting this valuable chance, I want to thank my classmates, friends and my family members for their consistent support.

And lastly I want to thank my parents and God for their consistent flow of energy by which we are able to do anything in this world.

Shashank Singh
July, 2009

Contents

List of Figures

Chapter 1

Introduction

Medical imaging is one of the powerful tool for gaining insight into the normal and pathological processes that affect health.Now a days the various imaging modalities, such as microscopy,computer tomography, ultrasound ,medical resonance imaging (MRI) and PET etc, are used in medical decision making processes and in surgical actions.Therefore high quality of accuracy is needed in taking the images .Clinical applications of a medical image require that image should be sufficiently clear and free from artifacts.That is why we need some preprocessing steps to remove the various image artifacts that comes due to imperfection in the image acquisition process.

In this work, a class of preprocessing step ,will be addressed ,that deals with a spurious smoothly varying image intensity, which is apparent in the images obtained by different imaging modalities such as microscopy,CT,ultrasound and above all in the magnetic resonance imaging.This spurious variation of intensity is known as intensity inhomogeneity, intensity non-uniformity or bias field.Basically I will address the intensity inhomogeneity in MRI s as the impact of this image technique in neurological applications is impressive, due to less side effects and flexibility in joining high-quality anatomical images with functional information.

1.1 Road-map of the report

In chapter 2, basic principle of MR Imaging is discussed .Here I have briefly covered the advantages and disadvantages of MRI s .Because of its usefulness for the soft tissues, it is widely used for taking the image of human brain . In chapter 3, intensity inhomogeneity ,its causes and the basic models of intensity inhomogene-

ity in Medical Resonance Imaging are discussed .Also the various approaches of intensity inhomogeneity correction are discussed. The summary of works done on bias field correction till today, is briefly covered in this chapter .

In chapter 4, a correction strategy is discussed ,which is based on expectation maximization and log likelihood estimation .Where I have given the complete mathematical setup of this approach and have highlighted the various issues such as the tuning of parameters of the algorithm, related to the algorithm

In chapter 5, **C-Means Clustering algorithm**, that is used in the estimation mean and variance of tissue classes, discussed .Both the Hard C-means and Fuzzy C-Means algorithms are discussed in detail .As these are used in inhomogeneity correction work for estimating mean and variance of tissue classes.

Chapter 6 consists of my core work ,where I have tried to tune the parameters of this correction approach using the bench marked data sets, I have put the results of my various experiments in which I used various strategies for estimating the parameters of the image and the bias field to optimize the performance of this algorithm.Estimated parameters are used to correct the real life MR images.Some examples of real MRI are also given iv this chapter.

Chapter 8 contains the Summary and Future scope of this work.And finally the appendix contains some of the c-code used for the experiment purposes.

Chapter 2

Basic Principle of MRI

Magnetic resonance imaging (MRI) is an imaging technique used primarily in medical settings to produce high quality images of the inside of the human body.It is based on the principle of Nuclear Magnetic Resonance.

2.1 Nuclear Magnetic Resonance

- All atoms consist of outer shells of negatively charged particles called electrons buzzing around in diffuse clouds, and a dense central portion called the nucleus.
- Some of these nuclei behave like small bar magnets and when placed in a powerful magnetic field about half line up in the direction of the magnetic field and about half line up in the opposite direction. The nuclei in opposing directions will cancel each other out but a few out of a million will not.
- By providing energy in the form of radio waves these tiny magnets can be caused to change orientation, to resonate absorbing energy at a resonance frequency that depends directly on the strength of the magnetic field.
- The frequency of this precession is described by the Larmor frequency. $w_0 = -\gamma H_0$

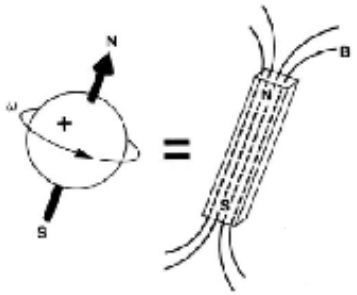

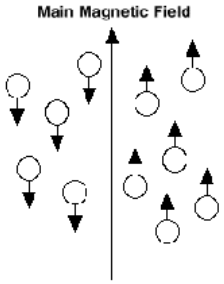

2.2 How would this work in the patient..

- When a patient is subject to a magnetic field (located straight down the center of the tube the patient is placed into) the H atoms in his/her body will line up in the direction of either his/her head or feet.
- The vast majority of the H+ will cancel each other out, but a couple out of a million will not.
- When an RF pulse specific to only H is applied to a specific part of the body being examined, the protons not cancelled out will absorb the energy required to make them spin or precess in a different direction a specific frequency called the Larmour frequency.
- The RF pulses are applied through a coil, designed for different parts of the body and conform to the contour of the body.

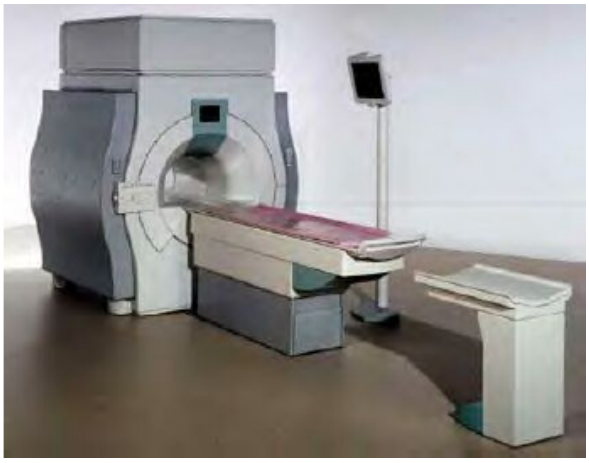

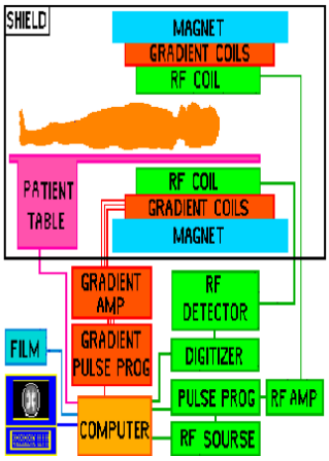

- By switching three small gradient magnets (18-27mT) on and off a variable magnetic field is formed.
- The large magnet immerses the patient in a stable and very intense magnetic field.
- By altering the gradient magnets, we can choose exactly which specific area of the body we want to analyze in slices.
- When the RF pulse is turned off, the H protons begin to slowly return to their natural alignment within the magnetic field and release their excess stored energy.
- The released energy, gives off a signal that the coil now picks up and sends to the computer system. The mathematical data is converted through the use of a Fourier transform, into a picture that we can put on film.

2.3 Sample MRI Slices

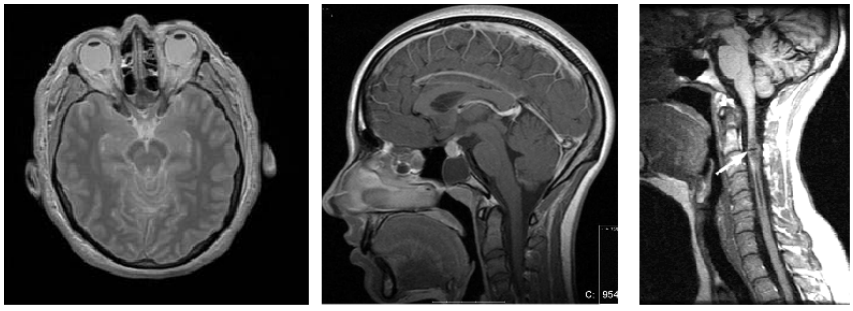

2.4 Advantages

- It does not use ionizing radiation.
- Very low incidence of side effects.
- Ability to image any plane: axial, sagitall, coronally
- Ideal for orthopedic and neurological applications.

2.5 Disadvantages

- Lower sensitivity then CT and X-Ray scans.
- Many people who can not be scanned by MRI because they have metal in their body or are too big to be scanned or are claustrophobic.
- Make a tremendous amount of noise. The stronger the main field, the louder the gradient noise.
- MRI scans require patients to hold still from 20 to 90 minutes or more. Very slight movement can cause very distorted images that will have to be repeated.
- Orthopaedic hardware (screws, plates, artificial joints) in the area of a scan can cause severe distortions on the images. The hardware causes a significant alteration in the main magnetic field.
- MRI systems are very expensive to purchase.

Chapter 3

Intensity Inhomogeneity

The images ,obtained by various medical image modalities such as Microscopy , CT ,Ultrasound and MRI, the intensity of same tissue varies with the location of the tissue , within the image .Which is due to the spurious smoothly varying image intensities , known as the intensity inhomogeneity or intensity non-uniformity or bias field.

Though the intensity inhomogeneity is hardly noticeable by human, many image analysis methods such as segmentation ,registration are highly sensitive to the spurious variation of image intensity.

Intensity inhomogeneity in MRI arises from the imperfection of the image acquisition process and manifest itself as a smooth intensity variation across the image sources of intensity inhomogeneity in MRI are generally divided int two groups:

- Sources in the first group are related to the properties of MRI device and include Static Field Inhomogeneity,Eddy Current driven by field gradient ,Radio Frequency transmission and reception inhomogeneity.
- Sources in the second group are related to imaged object itself ie to the shape ,position and orientation of the imaged object inside the magnet and the specific magnetic permeability and dielectric property of the subject .

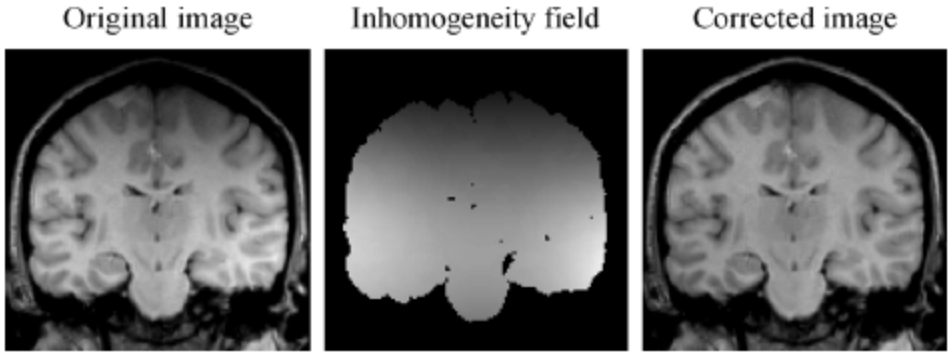

3.1 Models of intensity inhomogeneity

In its most simple form, the model assumes that intensity inhomogeneity is multiplicative or additive, i.e., the intensity inhomogeneity field multiplies or adds to the image intensities.Most frequently, the multiplicative model has been used as it is consistent with the inhomogeneous sensitivity of the reception coil.For modeling inhomogeneities that are due to induced currents and nonuniform excitation, the multiplicative model is less appropriate.

In addition to intensity inhomogeneity,the MR image formation model should incorporate noise,which can be approximated by a Gaussian distribution .In fact there are two types of noise :

- **Biological noise :** Corresponds to the within tissue inhomogeneity.
- **Scanner noise :** Which arises from MR device imperfections.

Let $u(x)$ be the inhomogeneity free image , $b(x)$ be the intensity inhomogeneity and $n(x)$ represent the noise incurred.

Model 1 : $v(x) = u(x)b(x) + n(x)$ (for scanner noise)

Model 2 : $v(x) = (u(x) + n(x))b(x)$ (for biological noise)

Model 3 : $log\ \ v(x) = log\ u(x) + n(x)$ (for log-transformed intensities)

In this dissertation work my aim is to estimate the bias field and to restore the MR image. I have considered the model based on log transformed intensities

, where the multiplicative inhomogeneity becomes the additive one . I have neglected the noise $n(x)$ and assumed that it is incorporated in the term $u(x)$. Before discussing the my approach let us first give the brief idea of all the inhomogeneity correction methods.

3.2 Classification of correction methods

Intensity inhomogeneity correction methods are broadly classified into two categories :

- **Prospective :** Aims at calibration and improvement of the image acquisition process.
- **Retrospective :** Based on the information of acquired image and apriori knowledge imaged object.

Retrospective methods are relatively general as only a few assumptions about the acquisition process are usually made. These methods mainly rely on the information of the acquired images in which useful anatomical information and information on the intensity inhomogeneity are integrated. A priori knowledge on spatial and/or intensity probability distribution of the imaged anatomy is used by some methods to facilitate extraction of information on intensity inhomogeneity. In contrast to the prospective methods, which can correct only the intensity inhomogeneity induced by an MR scanner, retrospective methods can also remove patient dependent inhomogeneity . The retrospective methods are further classified into :

- Filtering : Homomorphic Filtering
- Surface fitting : Intensity Based,Gradient Based
- Segmentation : ML, MAP Based,EM iterative scheme
- Histogram based : High-Frequency Maximization,Information Minimization
- Others

Filtering methods assume that intensity inhomogeneity is a low-frequency artifact that can be separated from the high-frequency signal of the imaged anatomical structures by low-pass filtering. Surface Fitting Methods fit a parametric surface to a set of image features that contain information on intensity inhomogeneity. The resulting surface, which is usually polynomial or spline based, represents the multiplicative inhomogeneity field that is used to correct the input image.

In segmentation based intensity inhomogeneity correction methods the two procedures ,bias correction and segmentation, are merged so that they benefit from each other, simultaneously yielding better segmentation and inhomogeneity correction

Histogram based methods operate directly on image intensity histograms and need little or no initialization and/or a priori knowledge on the intensity probability distribution of the imaged structures. This makes these methods fully automatic and highly general so that they can usually be applied to various images with or without pathology.

3.3 ML, MAP based intensity inhomogeneity correction method

This method uses maximum-likelihood (ML)or the maximum a posteriori probability (MAP) criterion to estimate the image intensity probability distribution.The models parameters are estimated by the expectation-maximization (EM) algorithm, iterating between classification and intensity inhomogeneity correction.For each tissue class in the brain MRI Gaussian distribution is taken .

I have used the above approach and basically followed the papers **Adaptive Segmentation of MRI Data** [1] and **Estimating the Bias Field of MR Images**[2] and estimated the various parameters of tissue classes of brain MR image .

Various algorithms are experimented for selecting the mean , variance ,and prior probabilities appropriately .Firstly I did my experiment on the simulated data and then applied the same algorithm with estimated parameters to real MRIs. I also tried to justify my results with physical explanations. In the next chapter I have covered the mathematical setup of the above two papers.

[1]W. M.Wells, III, W. E. L. Grimson, R. Kikins, and F. A. Jolezs, Adaptive segmentation of MRI data, IEEE Trans. Med. Imag., vol. 15, no.8, pp. 429-442, Aug. 1996.

[2]R. Guillemaud and M. Brady, Estimating the bias field ofMRimages,IEEE Trans. Med Imag., vol. 16, no. 3, pp. 238-251, Jun. 1997.

Chapter 4

Estimation of Intensity Inhomogeneity

In this chapter, I will discuss the **Wells *it al.*** and **Régis Guillemaud and Micahael Brady** techniques that use the maximum likelihood approach and EM algorithm to estimate the bias field .I experimented with these algorithms and standardize the parameters and found better correction with these estimated parameters.I will first discuss the basics of the algorithm :

As the goal is to estimate the multiplicative inhomogeneity ,Consider the inhomogeneity model based on the log transformed intensity .Now the inhomogeneity becomes additive in the transformed domain. Ignoring the noise $N(Y)$,that can be removed by prefiltering .

$$Y_i = \ln(X_i) \tag{4.1}$$

where X_i is the observed MRI signal intensity at the ith pixel.Y_i is the logarithm of pixel intensity X_i.Let $\beta(Y_i)$ denote the bias at ith pixel. Let n ne the total no of pixels.

Choose the set of classes (say: **white matter ,gray matter**,**air cerebro-spinal fluid** etc). Associate the jth tissue class with the Gaussian distribution on intensities Γ_j with mean μ_j and variance ψ_j .ie

$$p(Y_i|\Gamma_j) = G_{\psi_j}(Y_i - \mu_j) \tag{4.2}$$

Modifying Eq. (4.2) we get,

$$p(Y_i|\Gamma_j, \beta_i) = G_{\psi_j}(Y_i - \mu_j - \beta_i) \tag{4.3}$$

Let $p(\Gamma_j)$ represent the prior probability of tissue class Γ_j.Using the defnition of conditional probability , we may write

$$p(Y_i, \Gamma_j|\beta_i) = p(Y_i|\Gamma_j, \beta_i)p(\Gamma_j) \tag{4.4}$$

So conditional probability of intensity alone can be obtained by computing a marginal over tissue class

$$p(Y_i|\beta_i) = \sum_{\Gamma_j} p(Y_i, \Gamma_j|\beta_i) = \sum_{\Gamma_j} p(Y_i|\Gamma_j, \beta_i)p(\Gamma_j) \tag{4.5}$$

We assume the statistical independence of pixel intensities , so we can write the probability density of intire image as

$$p(Y|\beta) = \prod_i p(Y_i, \beta_i) \tag{4.6}$$

As the bias field varies slowly spatially.We can model it by a zero-mean Gaussian prior probability density

$$p(\beta) = G_{\psi_\beta}(\beta) \tag{4.7}$$

Next, Bayes' rule is used to obtain the posterior probability of the bias field, given the observed intensity data

$$p(\beta|Y) = p(Y|\beta)\frac{p(\beta)}{p(Y)} \tag{4.8}$$

where $p(Y)$ is an unimportant normalizing constant .
Having obtained the posterior probability on the bias field , we now use a maximum-a-posteriori(MAP) principle to formulate the estimate of bias field as the value of β having the **largest** posterior probability

$$\hat{\beta} = \arg \max_{\beta} \ p(\beta|Y) \tag{4.9}$$

A necessary condition for a maximum of posterior probability of β is that its gradient with respect to β be zero.We will use the equivalent zero gradient condition on the logarithm of the posterior probability

$$\left[\frac{\partial}{\partial\beta_i} \ \ln \ p(\beta|Y)\right]_{\beta=\hat{\beta}} = 0 \quad \forall \ i \tag{4.10}$$

Using eq. (4.6) and eq. (4.8) we get

$$\left[\frac{\partial}{\partial\beta_i}\left(\sum_j \ln p(Y_j|\beta_j) + \ln p(\beta)\right)\right]_{\beta=\hat{\beta}} = 0 \quad \forall\ i \tag{4.11}$$

Sinse only the ith term of the sum depends on β_i, we have (after differentiating the logarithms)

$$\left[\frac{\frac{\partial}{\partial\beta_i}p(Y_i|\beta_i)}{p(Y_i|\beta_i)} + \frac{\frac{\partial}{\partial\beta_i}p(\beta)}{p(\beta)}\right]_{\beta=\hat{\beta}} = 0 \quad \forall\ i \tag{4.12}$$

Using eq. (4.3) and eq. (4.5) , the above can be written as

$$\left[\frac{\sum_{\Gamma_j} p(\Gamma_j)\frac{\partial}{\partial\beta_i}G_{\psi_j}(Y_i-\mu_j-\beta_i)}{\sum_{\Gamma_j} p(\Gamma_j)G_{\psi_j}(Y_i-\mu_j-\beta_i)} + \frac{\frac{\partial}{\partial\beta_i}p(\beta)}{p(\beta)}\right]_{\beta=\hat{\beta}} = 0 \quad \forall\ i \tag{4.13}$$

Differentiating the Guassian expression in the first term yields

$$\left[\frac{\sum_{\Gamma_j} p(\Gamma_j)G_{\psi_j}(Y_i-\mu_j-\beta_i)\left[\psi_j^{-1}(Y_i-\mu_j-\beta_i)\right]}{\sum_{\Gamma_j} p(\Gamma_j)G_{\psi_j}(Y_i-\mu_j-\beta_i)} + \frac{\frac{\partial}{\partial\beta_i}p(\beta)}{p(\beta)}\right]_{\beta=\hat{\beta}} = 0 \quad \forall\ i \tag{4.14}$$

The expression may be more compactly written as

$$\left[\sum_j W_{ij}\left[\psi_j^{-1}(Y_i-\mu_j-\beta_i)\right] + \frac{\frac{\partial}{\partial\beta_i}p(\beta)}{p(\beta)}\right]_{\beta=\hat{\beta}} = 0 \quad \forall\ i \tag{4.15}$$

W_{ij} represents the probability that bias corrected pixel i belongs to tissue class j.

$$W_{ij} \equiv \frac{p(\Gamma_j)G_{\psi_j}(Y_i-\mu_j-\beta_i)}{\sum_{\Gamma_j} p(\Gamma_j)G_{\psi_j}(Y_i-\mu_j-\beta_i)} \tag{4.16}$$

Equation (4.15) may be re expressed as

$$\left[\sum_j W_{ij}\psi_j^{-1}(Y_i-\mu_j) - \sum_j W_{ij}\psi_j^{-1}\beta_i + \frac{\frac{\partial}{\partial\beta_i}p(\beta)}{p(\beta)}\right]_{\beta=\hat{\beta}} = 0 \quad \forall\ i \tag{4.17}$$

or as

$$\left[R_i - \Psi_i^{-1}\beta_i + \frac{\frac{\partial}{\partial \beta_i} p(\beta)}{p(\beta)} \right]_{\beta=\hat{\beta}} = 0 \quad \forall\ i \tag{4.18}$$

where R_i is known as mean residual :

$$R_i \equiv \sum_j W_{ij}\psi_j^{-1}(Y_i - \mu_j) \tag{4.19}$$

and

$$\Psi_i^{-1} \equiv \sum_j W_{ij}\psi_j^{-1} \tag{4.20}$$

Differentiating the last term in eq. (4.18) gives

$$R_i - \Psi_i^{-1}\hat{\beta}_i - \psi_\beta^{-1}\hat{\beta}_i = 0 \tag{4.21}$$

Finally the zero gradient condition for the bias field estimator may be concisely written as

$$\hat{\beta} = HR \tag{4.22}$$

Where the linear operator H is defined by

$$H \equiv \left[\Psi^{-1} + \psi_\beta^{-1} \right] \tag{4.23}$$

Finally, the EM algorithm is applied to (4.16) and (4.22) . Initially,the bias field is assumed to be zero everywhere. The equation (4.16) calculates the posterior tissue class probabilities W_{ij} (*Expectation step*).Using euation (4.19) we calculate R_i and then using eq. (4.22) we can find the bias field β_i.(*Maximization step*).

The abobe scheme is iterative one .I found that the β stablizes whithin 12 iterations .

4.1 Issues

There are various issues related to these algorithms :

- This method requires that MR intensity distribution should be modeled as a guassian mixure .Is it appropriate to model each tissue class as Gaussian distribution?

- How many tissue classes should be taken ? What is the impact of the number of tissue classes in the performence of the algorithm ?
- What algorithm should one use to get the better sigmentation of the tissue classes ?If we are modeling them by guassian distribution , How to choose their **mean** ,**variance** ?
- The algorithms needs the prior probability of tissue class . How to choose the prior probability of tissue classes to get the better performence ?
- Bias field is assumed to be guassian in this algo.How to choose the **mean** and **variance of bias** ?

For settling down the above issues I have experimented with the values of the paramenter needed and the various algorithms to work out the segmentation like issues. In the next chapter . I will provide the details of my experiment and its performence . In my experiment I noticed that if we take the number of tissue classes nearby 7 , we get the better result and increasing the number of tissue classes does not improve the result much ,which is quite true as there are 6 types of tissues in the brain , including the backgroud it becomes 7. For estimating the prior probability , mean and variance I observed that **K-Means Clustering Algorithm** gives the good result , as the k-mean clustering algorithm provides the natural clustering of the similar tisse class ,and with the knowledge of the number of pixels in a class , we can easily calculate the prior probabilities of the tissue class by the same algorithm.If we use the uniform prior probability , results are not at par with the results when the prior probabilities are calculated by above algorithm and which is quite natural.

Chapter 5

C-Means Clustering Algorithm

5.1 Hard C-Means

In clustering we intend to find out the **mutual grouping** existing in the data set .There are several ways to of formulating the defnition of natural grouping . THe process of clustering usually have the following steps :

1. Defining a measure of similarity or dissimilarity between the points .
2. Formulating an objective function .
3. Write an algorithm for obtaining the clusters satisfying (2)

Usually dissimilarity is measured by *distance function* . Usually we consider metrices for calculating distances .Similarity between two variables, sometimes is measured by the *angle* between the vectors corresponding to the variables.

5.1.1 Minimum within cluster distance criterion

Let $X = \{X_1, X_2, X_3, ..., X_t\}$ be the given data sets,
where $X_k = (X_{k1}, X_{k2}, X_{k3}, ..., X_{kn}) \in R^n$. Let the number of clusters c be known.A family $\{A_j : 1 \leq j \leq c\}$ is a c-partition of X iff,

- $\cup_{i=1}^{c} A_i = X$
- $A_i \cap A_j = \phi\,, \quad 1 \leq i \neq j \leq c$
- $\phi \subseteq A_j \subset X, \quad 1 \leq j \leq c$

Let *A*= $\{P(A_1, A_2, ...A_c) : P(A_1, A_2, ...A_c)\ is\ a\ partition\ of\ X\ \}$. Let for a partition $P(A_1, A_2, ...A_c)$,

$$Y_i = \frac{\left(\sum_{X \in A_i} X\right)}{\#(A_i)} \tag{5.1}$$

Let the objective function (loss function) is defined as

$$L(P(A_1, A_2, ..., A_c)) = \sum_{i=1}^{c} \sum_{X \in A_i} (\|X - Y_i\|)^2 \tag{5.2}$$

We would like to find $P(A_1^0, A_2^0, ..., A_c^0) \in A$, such that

$$L(P(A_1^0, A_2^0, ..., A_c^0)) \leq L(P(A_1, A_2, ..., A_c)) \quad \forall\ P(A_1, A_2, ..., A_c) \in A \tag{5.3}$$

We have suboptimal algorithm in literature for implementing this criterion .One such well known algorithm is **C-Means Algorithm** . There are several version of C-Mean Algorithm available in literature . One such version is given below .

5.1.2 C-means algorithm

1. Choose a partiton $P(A_{11}, A_{12}, .., A_{1c})$ of X into c classes.
   swhere $X = \{X_1, X_2, X_3, ..., X_t\} \subset R^n$ and c is number of classes.
2. $A_{21} = A_{22} = A_{23} = ... = A_{2c} = \phi$
3. Let Y_i = mean of A_{1i} , $i = 1, 2, 3, ..., c$
4. For $j = 1, 2, 3, .., t$. Put X_j into A_{2i} if $d(X_j, Y_i) \leq d(X_j, Y_i')$ for all $i' \neq i$ (Resolve ties arbitrarily)
5. If $A_{1i} = A_{2i} \forall i$ .Stop the algorithm, with the output as $A_{11}, A_{12}, ..., A_{1c}$ Otherwise rename A_{2i} as A_{1i} for all $i = 1, 2, 3, ..c.$ and Go to step (2).

Note :

- In order to create $A_{11}, A_{12}, ..., A_{1c}$ many authors considered c points say $Z_1, Z_2, ..., Z_c \in X$,(called seed points) ,and put all those X_is belonging to X in A_{1i} if the distance of X_i with Z_i are minimum .
- The algorithm usually converges.
- It is not necessary true that two different initial partitions (or two different set of seed points) give rise to the same final clustering .
- Usually the user decide the number of iteration in advance .

5.2 Fuzzy C-Mean

The objective of Fuzzy C-Mean algorithm is to partition a given data set into a certain number of natural and homogeneous sets where the element of each sets are similar as much as possible and dissimilar from those of other sets .
Let $X = \{X_1, X_2, X_3, ..., X_t\}$ be the given data sets,
where $X_k = (X_{k1}, X_{k2}, X_{k3}, ..., X_{kn}) \in R^n$.

5.2.1 Hard C-Partition

A family $\{A_j : 1 \leq j \leq c\}$ is a hard c-partition of X iff,

- $\cup_{i=1}^{c} A_i = X$
- $A_i \cap A_j = \phi\,, \quad 1 \leq i \neq j \leq c$
- $\phi \subseteq A_j \subset X, \quad 1 \leq j \leq c$

Let μ_{jk} be the menbership X_k to cluster to cluster A_j, $j = 1, 2, .., c$ and $k = 1, 2, ..., t$. For hard partitioning $\mu_{jk} \in \{0, 1\}$,Let V_{ct} be the set set of $c \times t$ matrices $2 \leq c < t$. Hard C-Partition for X is the set

$$M_c = \{U \in V_{ct} : \mu_{jk} \in \{0, 1\} \forall j, k \; and \; \sum_{j=1}^{c} \mu_{jk} = 1, \forall k, 0 < \sum_{k=1}^{t} \mu_{jk} < t\}$$

5.2.2 Fuzzy C-Partition

It is the set

$$M_c = \{U \in V_{ct} : \mu_{jk} \in [0,1]\, \forall j,k \; and \; \sum_{j=1}^{c} \mu_{jk} = 1, \forall k, 0 < \sum_{k=1}^{t} \mu_{jk} < t\}$$

e.g.

$$U = \begin{bmatrix} 0.91 & 0.42 & 0.67 \\ 0.09 & 0.58 & 0.33 \end{bmatrix}$$

5.2.3 Fuzzy C-Mean Algorithm

The objective of fuzzy c-mean algorithm is based on least squired error criterion .

Let $J_m : M_{fc} \times R^{cn} \rightarrow R^+$ be defined as

$$J_m(U,V) = \sum_{k=1}^{t} \sum_{j=1}^{c} (\mu_{jk})^m (d_{jk})^2 \tag{5.4}$$

where , $U \in M_{fc} \quad M_{fc}$ is a set of $c \times t$ matrices. $V = (v_1, v_2, v_3, ..., v_c) \in R^{cn}$ with $v_j \in R^n$ is the cluster center .$(d_{jk})^2 = (\parallel X_k - v_j \parallel)^2$ and weight component $m \in \{0, \infty\}$. Since each term of J_m is proportional to the $(d_{jk})^2$, J_m is a squire error clustering criterion and an infinite family of fuzzy clustering algorithm , one for each $m \in (0, \infty)$ is obtained via necessary conditions for solution of

$$\min_{M_{fc} \times R^{cn}} [J_m(U,V)] \tag{5.5}$$

Theorem 5.2.1. *Fix, $m \in \{0, \infty\}$, Lets X have at least $c < t$ distinct points and define $\forall k$ the sets ,*

$$I_k = \{j : 1 \leq j \leq c, d_{jk} = 0\}$$
$$\hat{I}_k = \{1, 2, ..., c\} - I_k$$

Then $(U,V) \in M_{fc} \times R^{cn}$ may be globally minimal for J_m only if ,

$$I_k = \phi \Rightarrow \mu_{jk} = \frac{1}{\sum_{j'=1}^{c} \left[\frac{d_{jk}}{d_{j'k}}\right]^{\frac{2}{m-1}}} \tag{5.6}$$

or

$$I_k \neq \phi \Rightarrow \mu_{jk} = 0 \quad \forall j \in \hat{I}_k \; and \; \sum_{j \in I_k} \mu_{jk} = 1 \tag{5.7}$$

and

$$v_j = \frac{\sum_{k=1}^{t} (\mu_{jk})^m X_k}{\sum_{k=1}^{m} (\mu_{jk})^m} \quad \forall j \tag{5.8}$$

Analysis : Eq. (5.6) is derived by fixing , $v \in R^{cn}$ and applying the Lagrange multiplier to the variables μ_{jk}. Eq. (5.7) is the alternate necessary form for membership of X_k, when there exist j so that $d_{jk} = 0$.This is called singularity and whenever it occurs , X_k must have no membership in any cluster , where $d_{jk} > 0$.Membership of X_k in cluster j ,where $d_{jk} = 0$, arbitrary up to column constraint.Singularity ie $X_k = v_j$ hardly occurs in practice .

Proof. First fix $V \in R^{cn}$ and define

$$g_m(U) = J_m(U, V) \tag{5.9}$$

for any $U \in M_{fc}$, so we have to find

$$\min_{U \in M_{fc}} [g_m(U)] = \min_{U \in M_{fc}} \left[\sum_{k=1}^{t} \sum_{j=1}^{c} (\mu_{jk})^m (d_{jk})^2 \right] \tag{5.10}$$

subject to

$$\sum_{j=1}^{c} \mu_{jk} = 1 \tag{5.11}$$

and

$$0 < \sum_{k=1}^{t} \mu_{jk} < t \tag{5.12}$$

If we avoid the constraint (5.12) , the columns of U are independent .For each column k of U let

$$g_{mk}(\mu_k) = \sum_{j=1}^{c} (\mu_{jk})^m (d_{jk})^2 \tag{5.13}$$

Let its Lagrangian be

$$F_k(\lambda, \mu_k) = \sum_{j=1}^{c} (\mu_{jk})^m (d_{jk})^2 - \lambda(\sum_{j=1}^{c} \mu_{jk} - 1) \tag{5.14}$$

For minimise F_k , we have

$$\frac{\partial}{\partial \lambda} F_k(\lambda, \mu_k) = 0 \Rightarrow \sum_{j=1}^{c} \mu_{jk} - 1 = 0 \tag{5.15}$$

and

$$\frac{\partial}{\partial \mu_k} F_k(\lambda, \mu_k) = 0 \tag{5.16}$$

this means

$$m(\mu_{jk})^{m-1}(d_{jk})^2 - \lambda = 0 \tag{5.17}$$

or

$$\mu_{jk} = \left[\frac{\lambda}{m(d_{jk})^2}\right]^{\frac{1}{m-1}} \tag{5.18}$$

Using Eq. (5.15)

$$\sum_{j'=1}^{c} \mu_{j'k} = 1$$

or

$$\sum_{j'=1}^{c} (\frac{\lambda}{m})^{\frac{1}{m-1}} \left[\frac{1}{(d_{j'k})^2}\right]^{\frac{1}{m-1}} = 1$$

or

$$(\frac{\lambda}{m})^{\frac{1}{m-1}} \sum_{j'=1}^{c} \left[\frac{1}{(d_{j'k})^2}\right]^{\frac{1}{m-1}} = 1$$

Thus

$$(\frac{\lambda}{m})^{\frac{1}{m-1}} = \frac{1}{\sum\limits_{j'=1}^{c} \left[\frac{1}{(d_{j'k})^2}\right]^{\frac{1}{m-1}}} \tag{5.19}$$

Putting the value in Eq. (5.19), we get

$$\mu_{jk} = \frac{1}{\sum_{j'=1}^{c} \left[\frac{d_{jk}}{(d_{j'k})^2} \right]^{\frac{2}{m-1}}} \tag{5.20}$$

□

Algorithm :

1. Fix c, $2 \leq c < t$ and fix $m \in (0, \infty)$ .Initialize $U^0 \in M_{fc}$ and $l = 0$.
2. $l = l + 1$ .Calculate the c-fuzzy cluster centers $\{v_j^l\}$ using Eq. (5.8).
3. Update U^l using Eq. (5.6) and Eq. (5.7).
4. Compare U^l with U^{l-1} in a convenient matrix norm ie if $\| U^l - U^{l-1} \| < \epsilon$ then stop ,otherwise return to step 2.

Fuzzy C-mean algorithm has the number of parameters ie : $c, m, U^0, \| \ . \ \|, \epsilon$ As $m \longrightarrow 1$ fuzzy c-mean converges to hard c-mean solution.Conversely as $m \longrightarrow \infty$, it is easy to see that $\mu_{jk} \longrightarrow (\frac{1}{c}) \forall j, k$ so $v_j \longrightarrow \mu$, the centroid of $X \ \ \forall j$.In general the larger m is , the fuzzier are the membership assignment and as m tends to 1 fuzzy c-mean solution becomes the hard.Weighting component m ,thus controls the extent of membership sharing between fuzzy clusters in$X$.

Chapter 6

Performence Analysis

6.1 Benchmark Data Sets

Here I have used the benchmark data sets where the ground truth is available .Using that I estimated the various parameters used in the algorithm.In the next section, these estimated parameters are used for correcting the real life magnetic resonance brain images.As in many natural processes, random variation conforms to the normal distribution,I will be using the normal distribution for the various tissue classes present in the brain MRI.The various parameters used in the algorithms are:

- Number of tissue classes in the brain MRI
- Prior probability of the tissue classes.
- Mean and Variance of the tissue classes.
- Mean and the variance of the intensity inhomogeneity.

As there are three types of MRIs, T1,T2,PD.I will be standardizing the above parameters for all the three types of MRIs. The various option for the above parameter are as under :

No. of Tissue Classes	Prior Prob. of tissue class	Mean and Variance	MRI type
6	Uniform prior probability	Using C-Mean Algorithms	T1
7	Prior Prob. Using C-Mean	Using fuzzy C-Mean	T2
more than 7	Background Uniform Prior Probability and other classes using C-mean	Manual Choice	PD

6.1.1 Standardizaion of number of tissue classes

Tissue classes visible in MRI scans include white and gray matter, cerebrospinal fluid (csf),menings (the protective membranes surrounding the brain),skull,muscle,fat,skin or air(see figure 6.1.1).Pathology introduces the addition classes of edema,tumer,hemorrhage, or other abnormality.

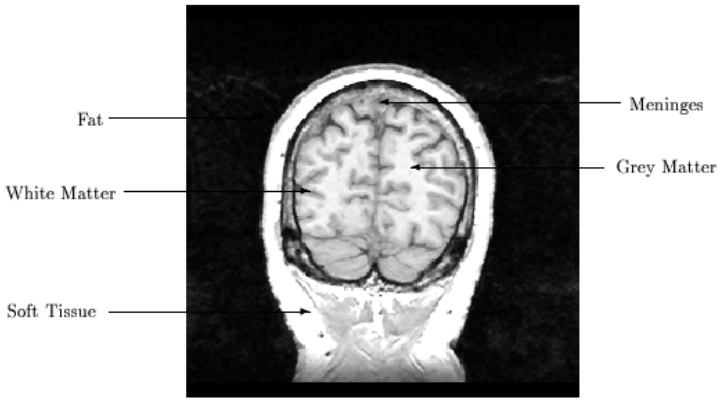

Figure 6.1: An Annotated Gradient Echo MR Slice (Air,CSF,Cranium are dark in this Image)

I have noticed that if we take number of tissue classes 8 or more , result of the above algorithm(in term of error in the biased corrected image) is almost same . While if we take the number of tissue class = 6 , results is slightly degraded .

Now in my further experiments, I will fix the number of tissue classes as 12 , using this much tissue classes , I will try to tune the prior probability of the various tissue classes present .

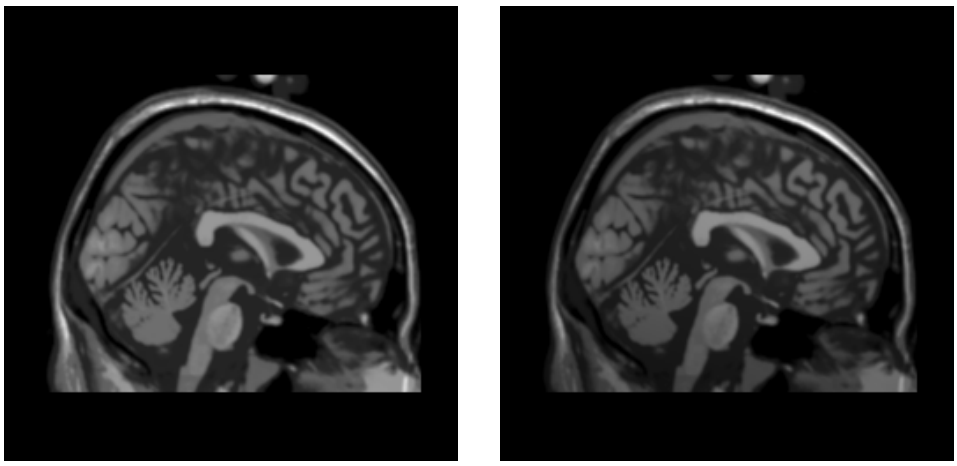

(a) bias free image (b) 40 % biased image

Figure 6.2: synthesized bias free and biased image

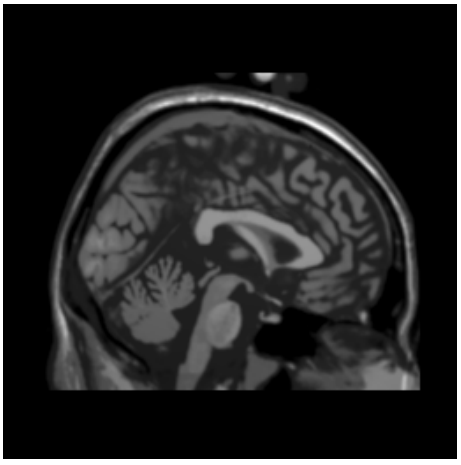

Figure 6.3: 20% biased mri brain image

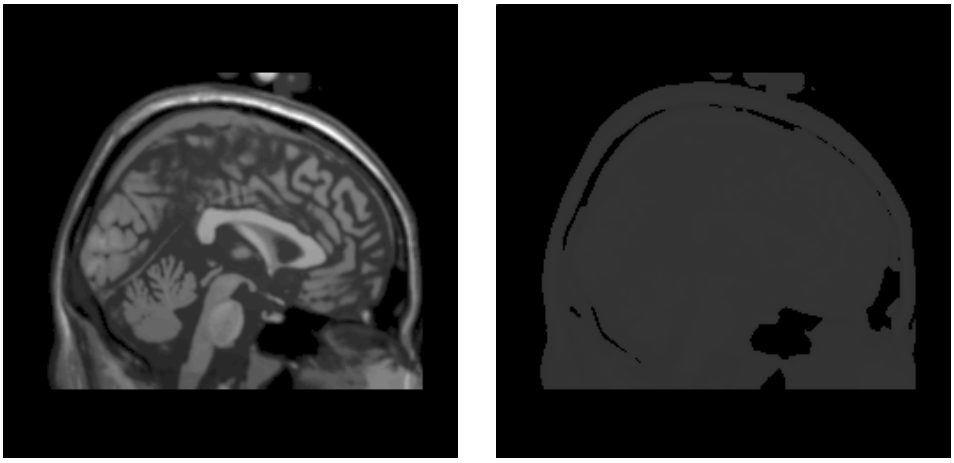

(a) corrected image (b) bias image

Figure 6.4: Corrected Image and its Bias Image where I have taken 10 number of tissue classes,actual image is biased by 40 %, I have choosen the other parameters using the c-mean clustering alghorithms and I have have taken bias image distribution to be Gaussian with zero mean and unit variance

Actual no of tissue class in mri(nc) : 10

Prior Prob	Mean	Variance
0.539165	-13.815511	0.000000
0.003110	0.348249	0.120693
0.001713	1.098613	0.000000
0.002975	1.497866	0.012511
0.008518	2.068077	0.032947
0.014678	2.653322	0.022055
0.064419	3.195009	0.015846
0.120621	3.595676	0.017528
0.118938	4.093898	0.019228
0.125864	4.587913	0.050694

Error in bias correction : 23.911566%

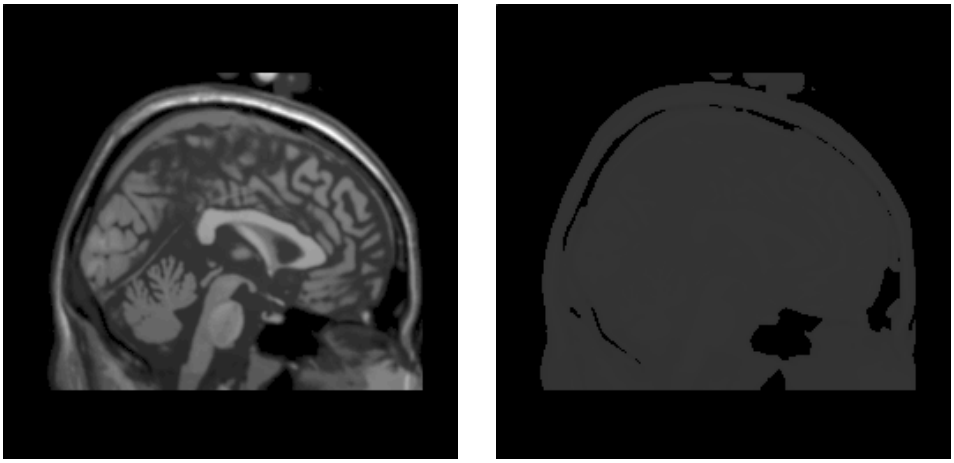

(a) corrected image (b) bias image

Figure 6.5: Corrected Image and its Bias Image where I have taken 8 number of tissue classes,actual image is biased by 40 %, I have choosen the other parameters using the c-mean clustering alghorithms and I have have taken bias image distribution to be Gaussian with zero mean and unit variance

```
Actual no of tissue class in mri(nc) : 8

============================================================
Prior Prob                Mean                      Variance
============================================================
0.539165                  -13.815511                0.000000
0.003110                  0.348249                  0.120693
0.006295                  1.464290                  0.070350
0.016045                  2.376317                  0.060083
0.061039                  3.134456                  0.022573
0.124797                  3.570483                  0.017972
0.123685                  4.083717                  0.021087
0.125864                  4.587913                  0.050694
============================================================
```

Error in bias correction : 23.911566%

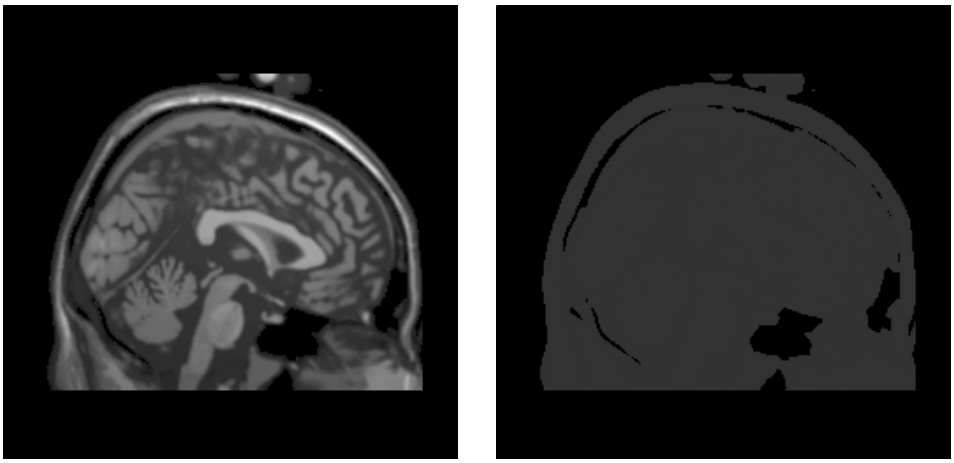

(a) corrected image (b) bias image

Figure 6.6: Corrected Image and its Bias Image where I have taken 6 number of tissue classes,actual image is biased by 40 %, I have chosen the other parameters using the c-mean clustering algorithms, and I have have taken bias image distribution to be Gaussian with zero mean and unit variance

```
Actual no of tissue class in mri(nc) : 6

============================================================
Prior Prob                Mean                      Variance
============================================================
0.539165                -13.815511                  0.000000
0.006310                0.796601                    0.265628
0.021663                2.326459                    0.126086
0.133435                3.332397                    0.036489
0.149630                3.929701                    0.034186
0.149796                4.538172                    0.055736
============================================================
```

Error in bias correction : 26.439083%

Now in my further experiments, I will fix the number of tissue classes as 12 , using this much tissue classes , I will try to tune the prior probability of the various tissue classes present .

6.1.2 Choice of prior probability of tissue classes

There are three option for choosing the prior probability

- Uniform prior probability
- Prior probability using C-Mean clustering algorithm
  - After the C-Mean algorithm is converged , We count the number of pixels belonging to a class.
  - Dividing the number of pixels in a class by total number of pixels in the image , we get the prior probability.
- Background some fixed prior probability and tissue class prior probability using c-mean

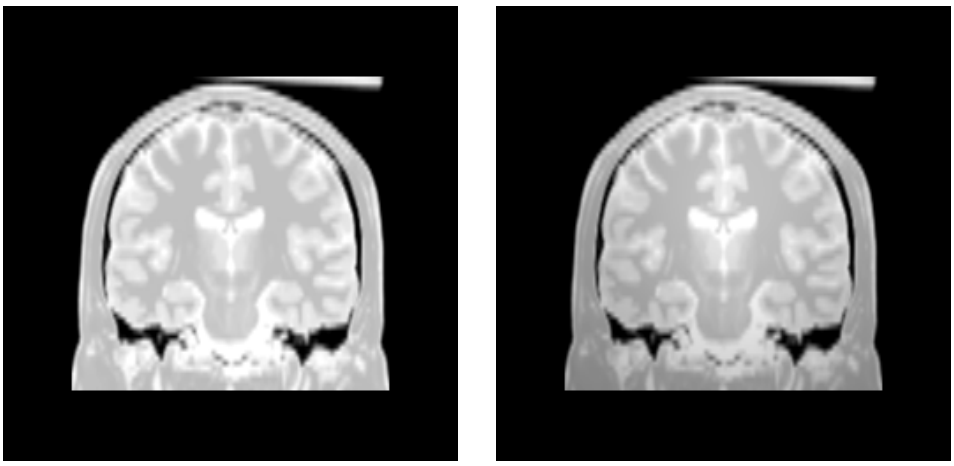

(a) bias free image (b) 40 % biased image

Figure 6.7: PD MRI,where the slice thickness is 3

I have noticed through my experiment that the various option for choosing the prior probability does not effect the performance of the algorithm any more .As one can see in the following table that we got the same percentage error in the

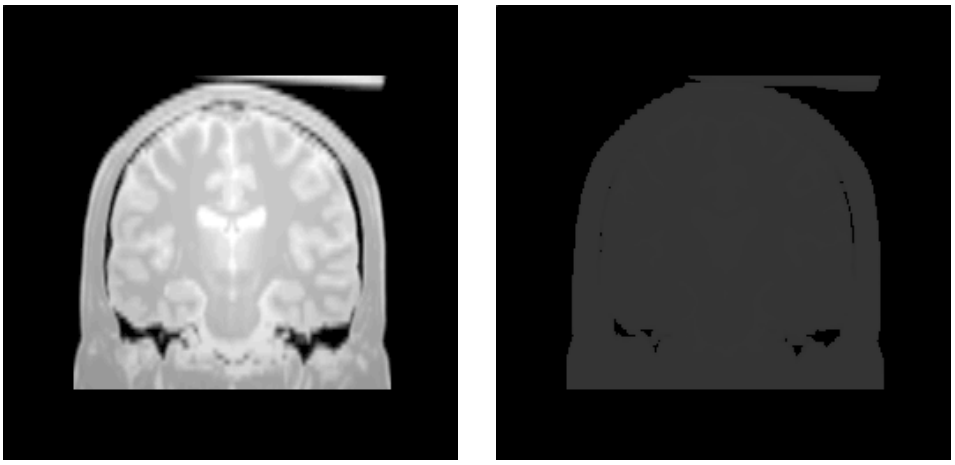

(a) bias free image (b) 40 % biased image

Figure 6.8: Bias corrected Image and corresponding bias

bias corrected image for both the cases one for uniform prior probability for all the classes and other when prior probability is measured by c-mean algorithm.

As the different choice of prior probability does not affect the performance . So henceforth we take the uniform prior probability and the number of tissue classes equal to 12.

```
Actual no of tissue class in mri(nc) : 10

============================================================
Prior Prob                 Mean                      Variance
============================================================
0.100000                -13.815511                   0.000000
0.100000                0.311028                    0.120393
0.100000                1.098613                    0.000000
0.100000                1.386295                    0.000000
0.100000                2.196069                    0.063679
0.100000                3.051826                    0.056805
0.100000                3.864688                    0.046232
0.100000                4.567406                    0.026804
0.100000                5.046362                    0.007393
0.100000                5.302212                    0.007441
============================================================
```

uniform prior probability

Error in bias correction : 14.285212%

```
Actual no of tissue class in mri(nc) : 10

============================================================
Prior Prob                 Mean                      Variance
============================================================
0.584625                -13.815511                   0.000000
0.001172                0.311028                    0.120393
0.000496                1.098613                    0.000000
0.000496                1.386295                    0.000000
0.003666                2.196069                    0.063679
0.005664                3.051826                    0.056805
0.009314                3.864688                    0.046232
0.015864                4.567406                    0.026804
0.115558                5.046362                    0.007393
0.263145                5.302212                    0.007441
============================================================
```

prior probability by c-mean

Error in bias correction : 14.285212%

6.1.3 Mean and Variance of tissue classes

Main difficulty with this algorithm is " how to choose the mean and variance of the tissue classes ? ".There are the various ways to choose the mean and hence variance of the tissue classes .I experimented with the following three algorithms of selecting means and variance.

- Manual Assignment
- Using C-Mean Algorithm
  - Random initialization
  - Manual initialization
- Using Fuzzy C-Mean Algorithm

I fixed the number of tissue classes equal to 12 and have taken the prior probability of tissue classes to be uniform . Through my experiment , I found that choosing mean and variance by C-Means Clustering algorithm gives the better result than that of by choosing fuzzy c-mean algorithm. In the first case where I have assigned the value of mean and variance of tissue classes manually ,sometimes I get good result and sometimes not. In the C-Means Approach , we can choose the initial means in two ways - one can assign the initial means by random pixel values or manually assign the initial means by observing the data properly . I observed that manual initialization of initial means gives the better results .

6.1.4 Result for C-mean Approach

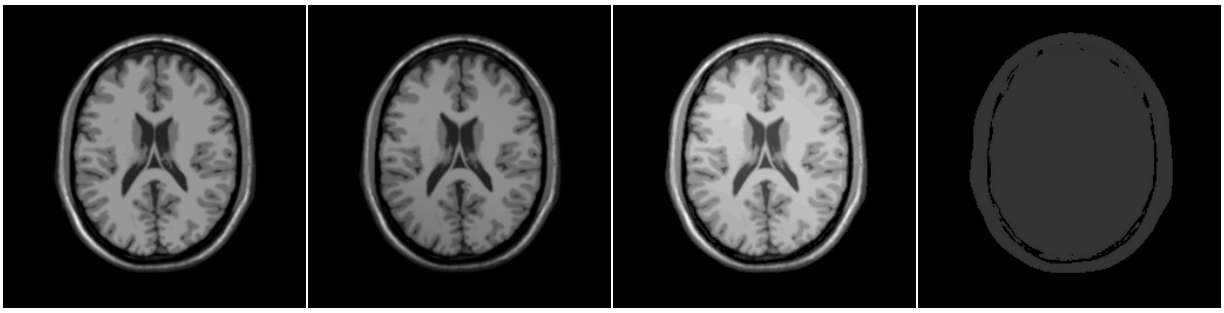

(a) Bias free Image (Ground Truth) (b) 40 % biased image (c) Bias Corrected Image (d) Bias field of Image

Actual no of tissue class in mri(nc) : 12

Prior Prob	Mean	Variance
0.083333	-13.815511	0.000000
0.083333	0.355282	0.120644
0.083333	1.098613	0.000000
0.083333	1.496794	0.012507
0.083333	2.020358	0.018271
0.083333	2.515819	0.016406
0.083333	3.026185	0.022826
0.083333	3.555173	0.019137
0.083333	4.072430	0.016921
0.083333	4.486561	0.007205
0.083333	4.710486	0.004867
0.083333	4.932666	0.003169

(e) Various parameters

Figure 6.9: Bias corrected Image and corresponding bias ,where the C-mean Algorithm is used to estimate mean and variance of tissue class ,and variance of bias is 1 .

6.1.5 Result for Fuzzy C-mean Approach

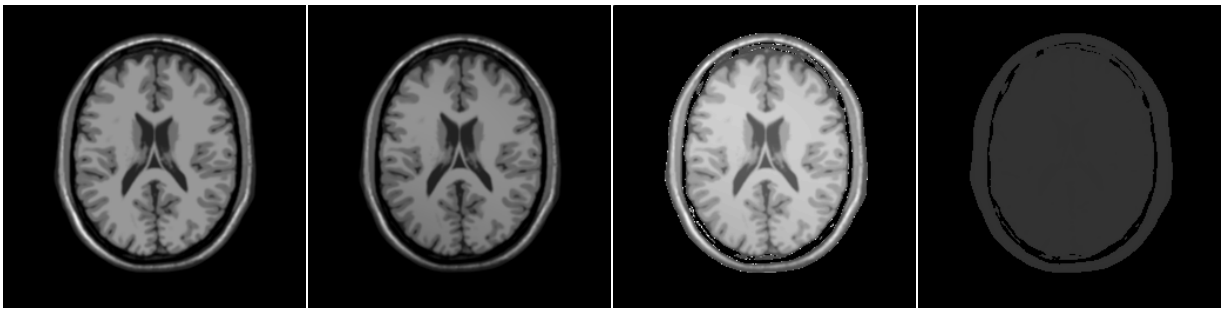

(a) Bias free Image (Ground Truth) (b) 40 % biased image (c) Bias Corrected Image (d) Bias field of Image

Actual no of tissue class in mri(nc) : 12

Prior Prob	Mean	Variance
0.083333	-13.823227	0.000000
0.083333	3.822767	2.369562
0.083333	3.712595	1.952074
0.083333	3.685204	1.985271
0.083333	3.023156	3.048047
0.083333	1.719256	2.893884
0.083333	1.808325	0.788940
0.083333	3.091295	0.320173
0.083333	3.564689	0.130740
0.083333	4.427962	0.066216
0.083333	4.816227	0.027518
0.083333	1.700191	1.736096

(e) Various parameters

Figure 6.10: Bias corrected Image and corresponding bias ,where the Fuzzy C-mean Algorithm is used to estimate mean and variance of tissue class ,and variance of bias is 1 .

Now ,C-mean Approach will be used to get the mean and the variance of tissue class.Taking the uniform prior probability and the number of tissue classes equal to 12 ,variance of the bias field will be standardized .

6.1.6 Estimating Variance of Bias

It is observed that the when the number of tissue classes is equal to 10 or more , unit variance of intensity inhomogeneity gives the proper error estimation .On the other hand when the number of tissue classes is less that 10 ,it is fit to take the variance of intensity inhomogeneity equal to 2.Following table gives the clear insight into the problem :

Table 6.1: table, showing the error estimates where I have taken a 20% biased mri and used uniform prior probability and calculated mean and variance using C-Mean Clustering algorithm

Number of Tissue Classes	**Error in Estimation (Variance of Bias Field=1)**	**Error in Estimation (Variance of Bias Field=2)**	**Error in Estimation(Variance of Bias Field=3)**
4	24.885973	24.825037	24.962784
6	23.768612	22.825037	23.843464
8	20.772009	21.267250	22.127800
10	20.772009	21.267250	22.127800
12	20.772009	21.267250	22.127800
14	20.772009	21.267250	22.127800
23	20.772009	21.267250	22.127800

As we see that variance of bias field in between 1 and 2 is appropriate .

Variance of bias field=1

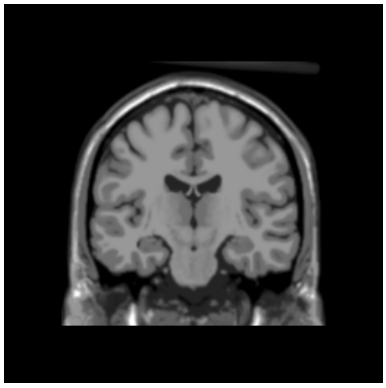

(a) ground truth

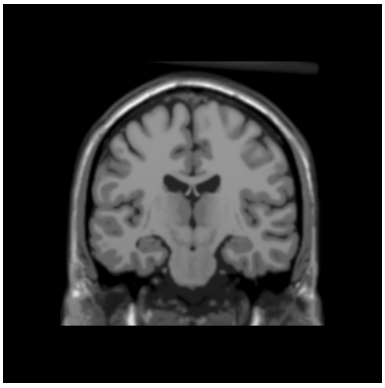

(b) 20% biased image

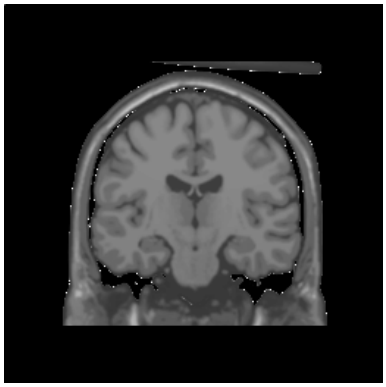

(c) corrected image (no of tissue classes=4,error=24.885973)

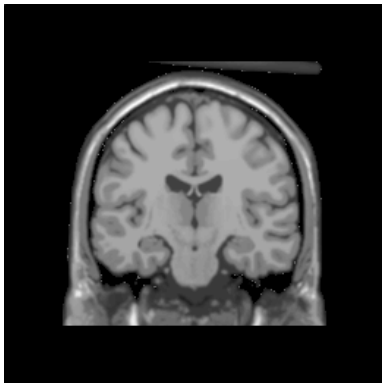

(d) corrected image (no of tissue classes=6,error=23.768612)

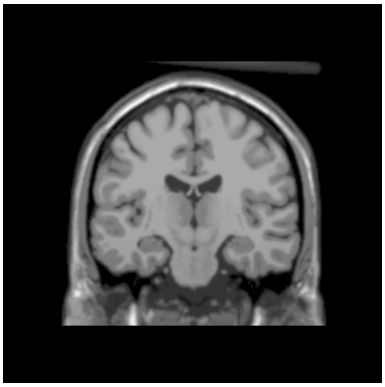

(e) corrected image (no of tissue classes=8,error=20.772009)

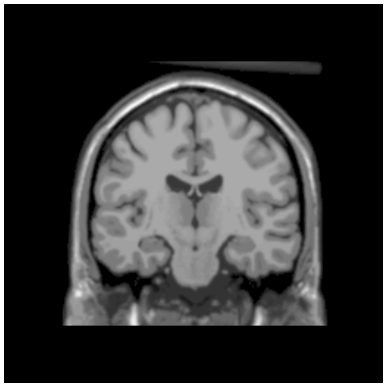

(f) corrected image (no. of tissue classes=10,error=20.772009)

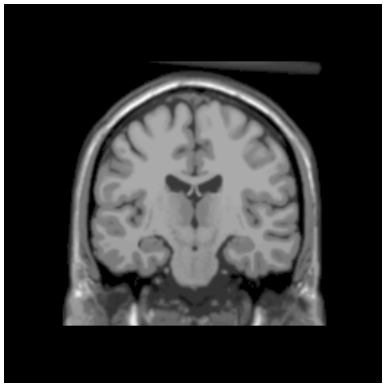

(g) corrected image (no of tissue classes=12,error=20.772009)

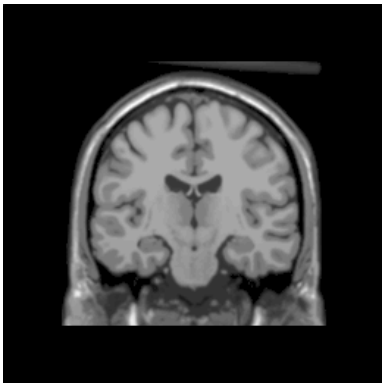

(h) corrected image (no of tissue classes=23,error=20.772009)

Figure 6.11: Bias corrected images where variance of bias field =1

6.1.7 Result for various modalities

Medical resonance imaging technique is capable of taking three types of images : T1, T2, PD.Above correction strategy works for all the three modes of this imaging technique.For PD MRI s the above standardized parameters works better than that of T2, and T1 MRI s.For T2 MRI s the above standardized parameters works better than that of T1 MRI s.

PD MRI, Error :20.996656 %

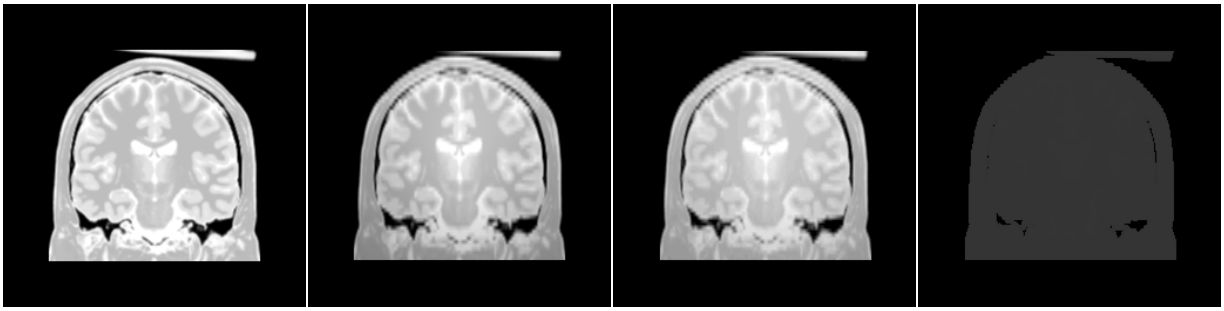

(a) ground truth (b) 40% biased image (c) bias corrected (d) bias

T1 MRI, Error :27.048025%

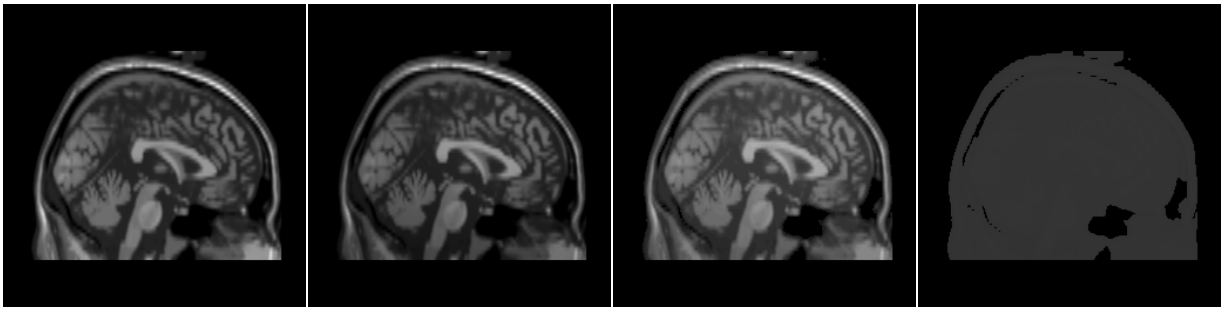

(e) ground truth (f) 40% biased image (g) bias corrected (h) bias

T2 ,MRI, Error :17.510017 %

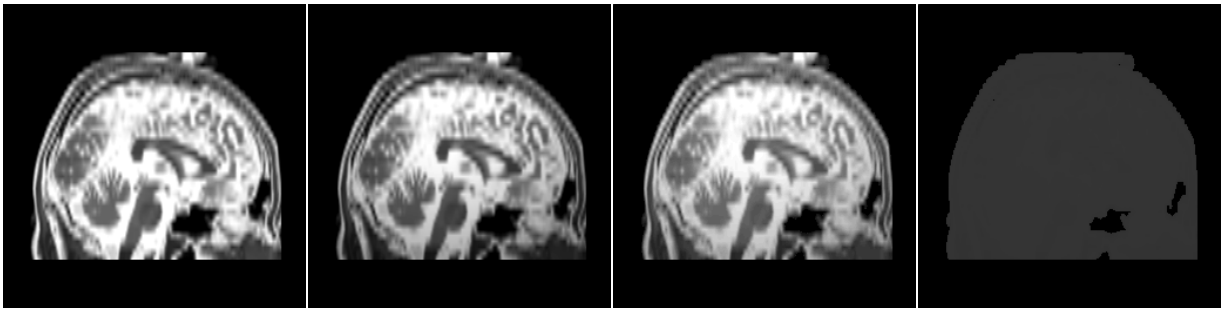

(i) ground truth (j) 40% biased image (k) bias corrected (l) bias

Figure 6.12: Bias corrected images for different modalities

6.2 Real Life Data Set

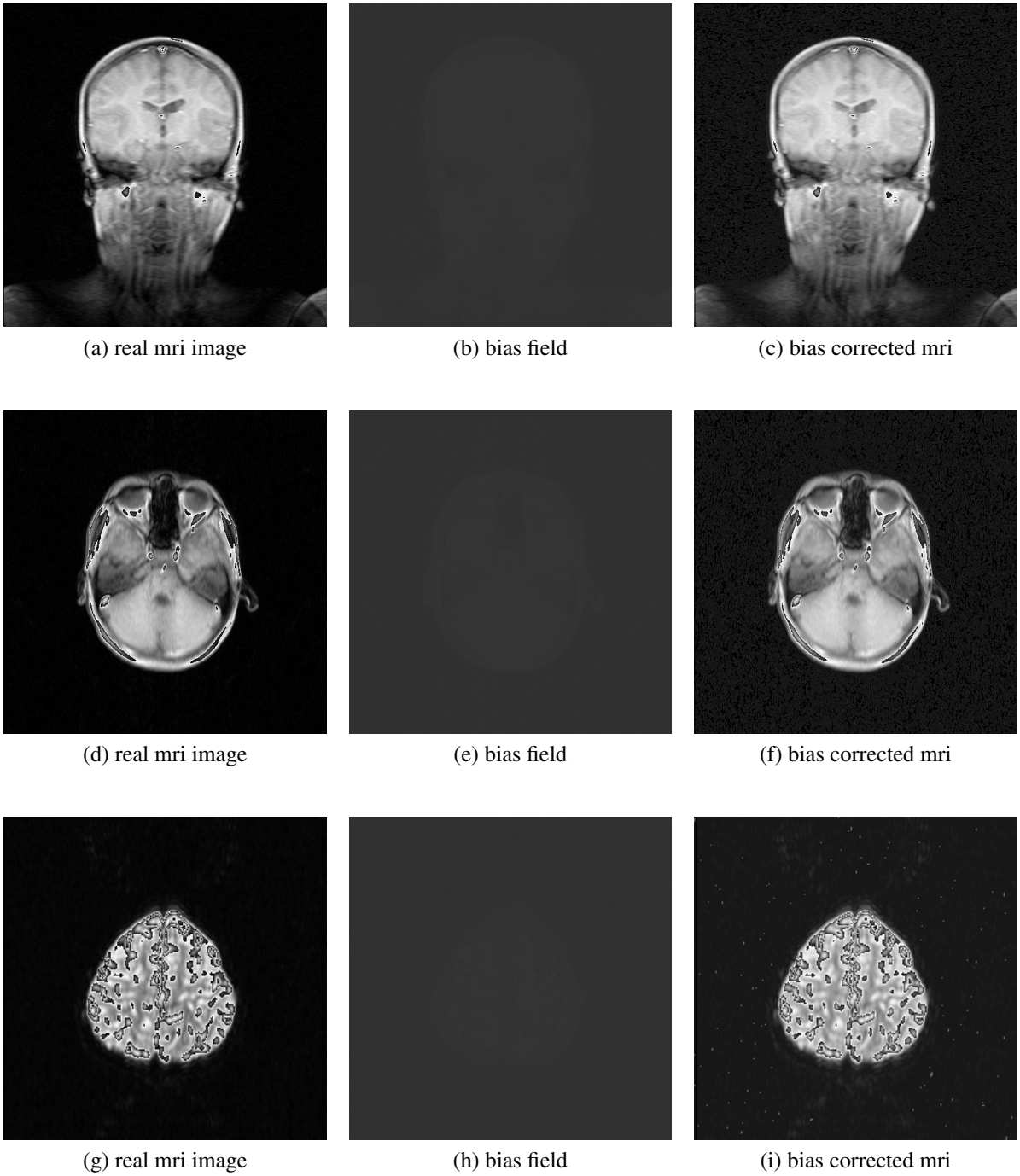

(a) real mri image (b) bias field (c) bias corrected mri

(d) real mri image (e) bias field (f) bias corrected mri

(g) real mri image (h) bias field (i) bias corrected mri

Figure 6.13: Bias corrected real mris images

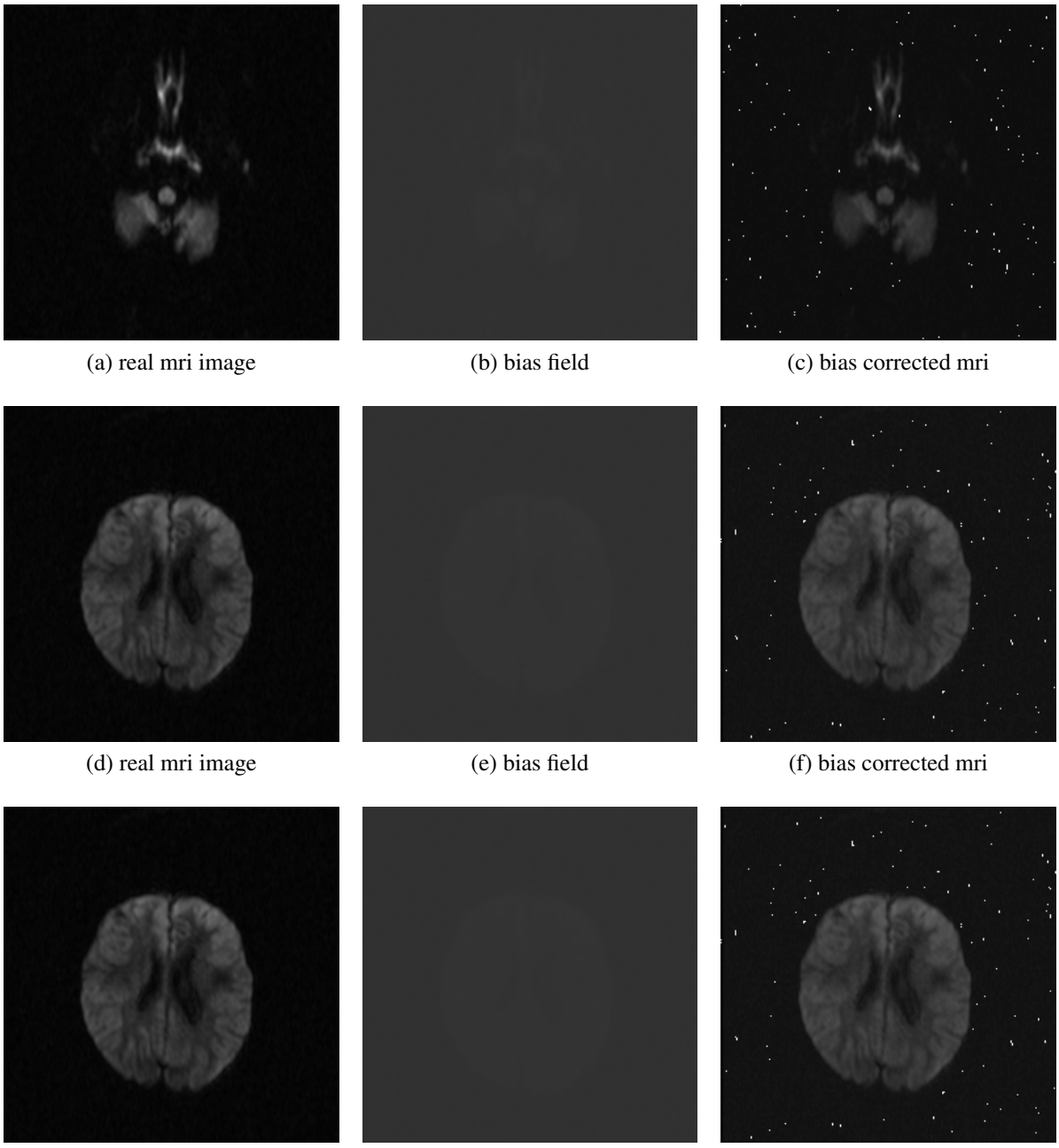

(a) real mri image (b) bias field (c) bias corrected mri

(d) real mri image (e) bias field (f) bias corrected mri

(g) real mri image (h) bias field (i) bias corrected mri

Figure 6.14: Bias corrected real mr images

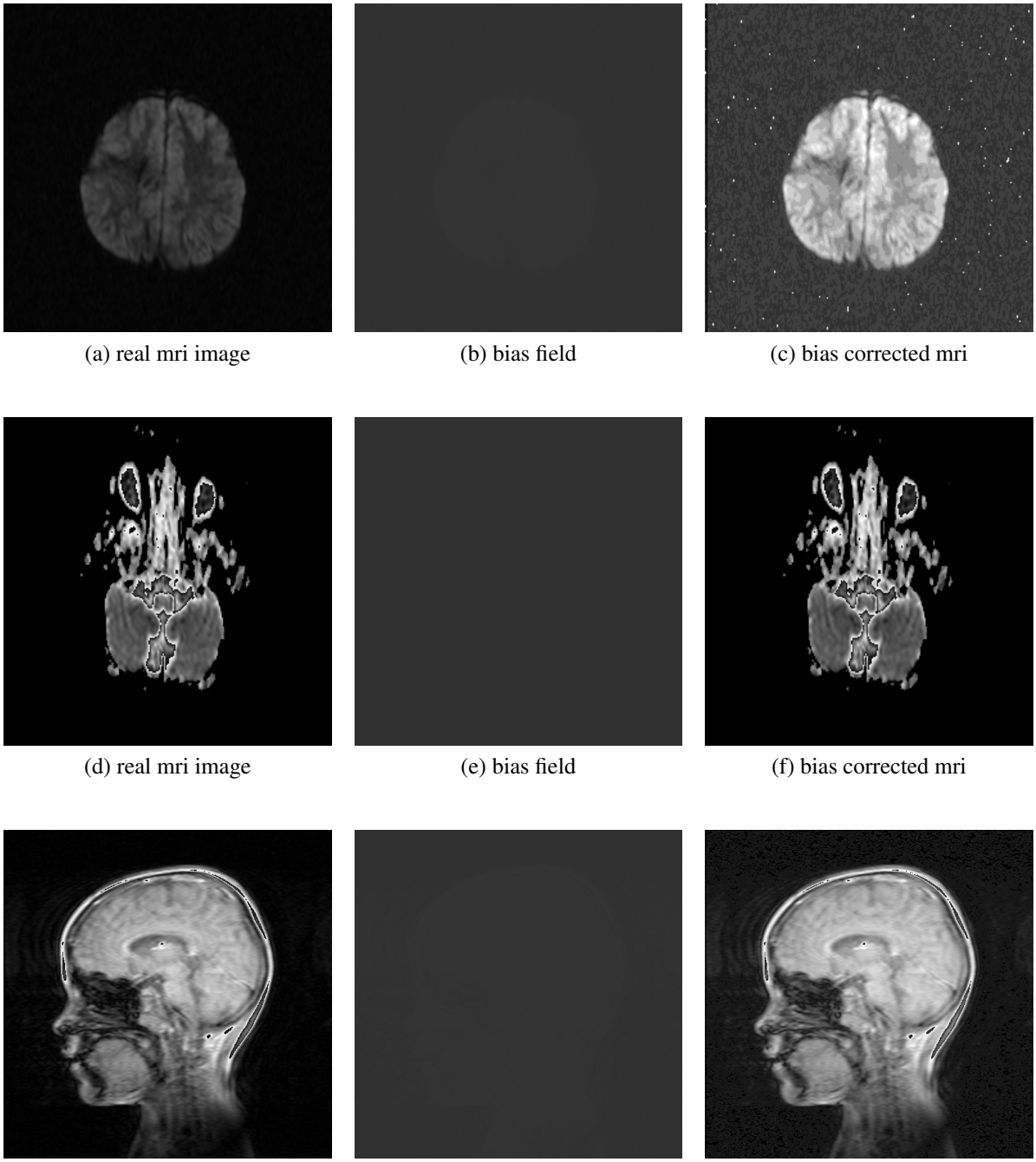

(a) real mri image (b) bias field (c) bias corrected mri

(d) real mri image (e) bias field (f) bias corrected mri

(g) real mri image (h) bias field (i) bias corrected mri

Figure 6.15: Bias corrected reals imagess

Chapter 7

Summary and Future Work

7.1 Summary

The algorithm used in this work works well for the brain MRIs , provided we choose the parameters properly . After all the experiment , it can be concluded that if we take number of tissue classes in between 12 to 20 , prior probability of tissue classes to be uniform , calculate the mean and variance of the tissue classes using C-mean clustering algorithm and take the variance of bias field in between 1-2 , the above algorithm works well and removes the intensity inhomogeneity of mri image to a satisfactory level.

7.2 Future Work

Problem of Intensity Inhomogeneity Correction is still alive.We have put some efforts to standardize the parameters of two existing algorithms ,still we are getting 20% of error in the bias correction .There is a scope to modify these algorithms further to have better error correction.One can study the brain anatomy and can work out the proper distribution of tissue classes present in the brain MR images .

Appendices

Appendix A

C-Code

A.1 bias.c

```
//shashank singh
//Roll No MTC0721
//ISI Kolkata

// This program only accept the "PGM" images
// and outputs in the PGM format

//compile this by "c99 bias.c -ln -Duniformpp"
//Use the appropriate preprosessor directive during compilation
//resultant images are created in the currect directory

#include<stdio.h>
#include<stdlib.h>
#include<math.h>
#include<string.h>

#define MAX 700
#define M 330
#define pi 3.1415
#define WS(x) (x==' '||x=='\n'||x=='\t'||x=='\r') //white spaces
#define epsln .0001

int pixel[MAX][MAX];  //pixel read from pgm brain image
int row,col,maxval,nc;  //nc=no of classes in the brain mri image
int c[MAX][MAX];  //class level
//int beta[MAX][MAX];
long double a[MAX][MAX],w[MAX][MAX][M],R[MAX][MAX],beta[MAX][MAX];
  // a(i,j)     -> log(pixel)
  // beta(i,j)  -> bias of image
```

```
  // w(i,j,k)   -> prob that pixel(i,j) belongs to class k
  // R          -> residual

long double m[M],v[M],P[M],prev_m[M];
  // m(i)  -> mean of class i
  // v(i)  -> variance of class i
  // P(i)  -> prior probability of class i
  // vbeta -> variance of bias

float vbeta; // variance of bias field

void remcomment(FILE**);

//using c-mean calculates the mean and variance
void calculate_classlevel_variance();
long double dist(long double ,long double);
//guassian distribution
long double  gpdf(long double ,long double ,long double);

//function calculates the bias field
void find_bias();
void enhance_pgm();

//stopping criterion of c-mean algo
int check_mean_stablisation();
int main()
{
  int i,j,k,iteration,zero=0;
  char MagicChar[M],temp,image[40],imagetmp[40];

  FILE *infp,*outfp,*bfp,*cfp;
  int flag1,flag2=0,iter,len,ftmp;


  printf("\n\tEnter the name of biased mri image : ");
  scanf("%s",image);

  //opening of MRI Image in PGM format
  infp=fopen(image ,"r");

  if(!infp)
  {
    printf("\nError in openning the input image  file !!\n");
    exit(1);
  }
```

```
fscanf(infp,"%s",MagicChar);
remcomment(&infp);
fscanf(infp,"%d",&row);
remcomment(&infp);
fscanf(infp,"%d",&col);
remcomment(&infp);
fscanf(infp,"%d",&maxval);

printf("\n\tMagic char = %s ,
 row= %d ,col=%d ,maxval=%d\n\n",MagicChar,row,col,maxval);


if((strcmp(MagicChar,"P5")))
{
  printf("\nInput Image in not in PGM Format !!\n");
  exit(1);
}

printf("\tEnter the no of iteration          : ");
scanf("%d",&iteration);

printf("\n\tEnter the  variance of bias field    : ");
scanf("%f",&vbeta);

printf("\n");

//Reading image into pixel
for(i=0;i<row;i++)
  for(j=0;j<col;j++)
  {
    fscanf(infp,"%c",&temp);
    pixel[i][j]=(unsigned char)temp;

    a[i][j]=logl((long double)pixel[i][j]+.000001);

    //printf("%f\t,",(double)a[i][j]);
  }

fclose(infp);

nc=30;//no of class

#ifndef finerinimean//use it if no of tissue classes > 20
#ifndef randinimean
```

```
  //initialisation of mean
  printf("\tEnter the no of tissue class(12< nc < 18): ");
  scanf("%d",&nc);
  for(i=0;i<nc;i++){
    m[i]=i-i*.5;
  //  m[i]=i;
     prev_m[i]=0;
  }
  #endif
  #endif

  #ifdef randinimean
  //random initialisation of mean
  printf("\tEnter the no of tissue class(nc < 50): ");
  scanf("%d",&nc);
  srand(getpid());
  for(i=0;i<nc;i++)
    m[i]=a[rand()%row][rand()%col];
  #endif

  #ifdef finerinimean //use it if no of tissue classes > 20
  printf("\tEnter the no of tissue class(30< nc < 50): ");
  scanf("%d",&nc);
  for(i=0;i<nc;i++)
    m[i]=i-i*.85;

  #endif


  for(i=0;i<nc;i++)
     printf("\t mean[%d]\t:%f\n",i,(double)m[i]);
//=====================================================================
  flag1=1;iter=0;
  while(flag1 && (iter < 50))
  {
     calculate_classlevel_variance();
     flag1=check_mean_stablisation();
     iter++;
  }
  printf("\n\tNo of iteration for mean convergence : %d\n",iter);
  printf("\n\tActual no of tissue class in mri(nc) : %d\n",nc);

//=====================================================================
  //printing of clustered image
  #ifdef cimage
```

```
    strcpy(imagetmp,image);
    len = strlen(imagetmp);
    imagetmp[len-4]='_';
    imagetmp[len-3]='c';
    imagetmp[len-2]='1';
    imagetmp[len-1]='s';
    imagetmp[len]='t';
    imagetmp[len+1]='\0';

    strcat(imagetmp,".pgm");

    cfp=fopen(imagetmp,"w");

    fprintf(cfp,"%s %d %d %d\n","P5",row,col,maxval);

    for(i=0;i<row;i++)
      for(j=0;j<col;j++){
        ftmp=(float)c[i][j]*255/(nc-1);
        fprintf(cfp,"%c",(unsigned int)ftmp);
        //printf("%d,",ftmp);
      }
    fclose(cfp);
    #endif

//=====================================================================

    #ifdef uniformpp
    //assigning uniform prior probability
    for(i=0;i<nc;i++)
      P[i]=(float)1/nc;
    #endif



    printf("\n\t=============================================================\n");
    printf("\tPrior Prob \t\t Mean \t\t\t Variance");
    printf("\n\t=============================================================\n");
    for(i=0;i<nc;i++){
      //P[i]=(long double)1/nc;
      printf("\t%f\t \t%f\t\t %f\n",(double)P[i],(double)m[i],(double)v[i]);
    }
    printf("\t=============================================================\n");
    printf("\n");

    for(i=0;i<iteration;i++)
```

```
  find_bias();


len = strlen(image);
image[len-4]='_';
image[len-3]='b';
image[len-2]='i';
image[len-1]='a';
image[len]='s';
image[len+1]='\0';

strcat(image,".pgm");

outfp=fopen(image,"w");

fprintf(outfp,"%s %d %d %d\n","P5",row,col,maxval);

for(i=0;i<row;i++)
  for(j=0;j<col;j++)
  {
    if(beta[i][j] > 0){
      fprintf(outfp,"%d",(unsigned int )nearbyint(beta[i][j]));
      //printf("%f\t",nearbyint(beta[i][j]));
      pixel[i][j]=(int)nearbyint(pixel[i][j]/beta[i][j]);
    }
    else
    {
      fprintf(outfp,"%d",(unsigned int)zero);
      //printf("%f\t",(double)zero);
    }

  }

fclose(outfp);

//enhancing the pixel[][]
enhance_pgm();


len = strlen(image);
image[len-4]='_';
image[len-3]='c';
image[len-2]='o';
image[len-1]='r';
image[len]='r';
```

```
  image[len+1]='e';
  image[len+2]='c';
  image[len+3]='t';
  image[len+4]='e';
  image[len+5]='d';
  image[len+6]='\0';

  strcat(image,".pgm");


  bfp=fopen(image,"w");
  fprintf(bfp,"%s %d %d %d\n","P5",row,col,maxval);
  for(i=0;i<row;i++)
    for(j=0;j<col;j++)
      fprintf(bfp,"%c",pixel[i][j]);

  fclose(bfp);



  return 0;

}

//for removing comment in PGM file
void remcomment(FILE **fp)
{
  char ch,buff[100];
        while(1)
        {
          ch=fgetc(*fp);
                while(WS(ch))
                  ch=fgetc(*fp);
                if(ch=='#')
                  fgets(buff,100,*fp);
                else break;
        }
        ungetc(ch,*fp);
}

//calculating distance between 2 number
long double dist(long double x,long double y)
{
  long double tmp;
  tmp=x-y;
```

```
  if(tmp > 0)
    return tmp;
  else
    return -tmp;
}


//for calculating class level and mean and variance of each class
void calculate_classlevel_variance()
{
  int i,j,k,l,no[M];
  long double dd[M],min,sum1[M],sum2[M];

  //initialisattion
  for(k=0;k<nc;k++){
    sum1[k]=sum2[k]=0;
    no[k]=0;
    dd[k]=0;
  }

  //assign class labels
  for(i=0;i<row;i++)
    for(j=0;j<col;j++)
    {
      for(k=0;k<nc;k++)
        dd[k]=dist(a[i][j],m[k]);

      min=dd[0];l=0;
      for(k=1;k<nc;k++)
      {
        if(min > dd[k])
        {
          min=dd[k];
          l=k;
        }
      }

      c[i][j]=l;//class label
      //printf("%d\t",l);
    }

  //modified mean and variance
  for(i=0;i<row;i++)
    for(j=0;j<col;j++)
    {
```

```
        sum1[c[i][j]] += a[i][j];
        no[c[i][j]]++;
      }


  //mean and prior probability calculation
  for(k=0;k<nc;k++){
    m[k]=sum1[k]/no[k];
    P[k]=(long double)no[k]/(row*col);
  }

  for(i=0;i<row;i++)
    for(j=0;j<col;j++)
      sum2[c[i][j]] +=(a[i][j]-m[c[i][j]])*(a[i][j]-m[c[i][j]]);

  //variance calculation
  for(k=0;k<nc;k++)
    v[k]=sum2[k]/(no[k]-1);



  i=0;j=0;
  while(i<nc)
  {
    if(no[i]== 0)
      i++;
    else
    {
      m[j]=m[i];
      v[j]=v[i];
      P[j]=P[i];
      i++;
      j++;
    }
  }
  nc=j;

}

long double  gpdf(long double x ,long double mean ,long double var)
{
  return expl(-(((x-mean)*(x-mean))/(2*var)))/(sqrt(2*pi*var));
}

void find_bias()
```

```
{
  int i,j,k;
  long double sm1,sm2,tmp;

  for(i=0;i<row;i++)
    for(j=0;j<col;j++)
    {
      R[i][j]=0;
      sm1=0,tmp=0;
      for(k=0;k<nc;k++)
        sm1 += P[k]*gpdf(a[i][j]-m[k]-beta[i][j],m[k],v[k]);

      for(k=0;k<nc;k++){
        tmp=P[k]*gpdf(a[i][j]-m[k]-beta[i][j],m[k],v[k]);
        w[i][j][k]=tmp/(sm1);
        R[i][j] +=w[i][j][k]*(a[i][j]-m[k])/v[k];
      }

      //printf("%f\t",(double)R[i][j]);
    }



  for(i=0;i<row;i++)
    for(j=0;j<col;j++)
    {
      sm2=0;
      for(k=0;k<nc;k++)
        sm2 +=w[i][j][k]/v[k];

      sm2=sm2+((long double)1/vbeta);
      //printf("%f\t",(double)(R[i][j]));

      beta[i][j]=( R[i][j]/sm2);


    }
}

void enhance_pgm()
{
  int i,j,k;
  int aa,bb,cc;
  float tmp;
  FILE *fp;
```

```
  aa=pixel[0][0];
  bb=pixel[0][0];

  for(i=0;i<row;i++)
    for(j=0;j<col;j++)
    {
      if(aa > pixel[i][j])
        aa=pixel[i][j];

      if(bb < pixel[i][j])
        bb=pixel[i][j];
    }

  for(i=0;i<row;i++)
    for(j=0;j<col;j++){
      tmp=((float)255/(bb-aa))*(pixel[i][j]-aa);
      pixel[i][j]=(int)tmp;
    }

}

int check_mean_stablisation()
{
  int i,flag;
  long double aaa;
  flag=0;
  for(i=0;i<nc;i++)
  {
    aaa=m[i]- prev_m[i];
    if((aaa > 0 && aaa > epsln) || (aaa < 0 && (-aaa) > epsln))
      flag=1;

    prev_m[i]=m[i];
  }
  return flag;
}
```

A.2 error.c

```
//shashank singh
//Roll No MTC0721

// This will calculate the error in the corrected image
// and the actual image (if available)

#include<stdio.h>
#include<stdlib.h>
#include<math.h>
#include<string.h>

#define MAX 1000
#define M 50
#define epsln 20
#define WS(x) (x==' '||x=='\n'||x=='\t'||x=='\r')

int a[MAX][MAX],b[MAX][MAX];//a -> actual pixel ,b-> corrected pixel
int row1 ,col1,maxval1,row2,col2,maxval2;
char MagicChar1[M], MagicChar2[M];


void remcomment(FILE **);
void APE();
void error_image();
int main()
{
  int i,j,k;
  char image1[M],image2[M];
  char tmp1,tmp2;

  FILE *fp1,*fp2;


  printf("\n\tEnter the name of bias free image : ");
  scanf("%s",image1);
  printf("\n\tEnter the name of bias_corrected image : ");
  scanf("%s",image2);

//   image1="b0.pgm";image2="bias_free.pgm";

  //opening of MRI Image in PGM format
  fp1=fopen(image1 ,"r");
  fp2=fopen(image2 ,"r");
```

```
if(!fp1)
{
  printf("\nError in openning the
             input image  file : %s !!\n",image1);
  exit(1);
}
if(!fp2)
{
  printf("\nError in openning the
             input image  file : %s !!\n",image2);
  exit(1);
}

fscanf(fp1,"%s",MagicChar1);
fscanf(fp2,"%s",MagicChar2);

remcomment(&fp1);
remcomment(&fp2);

fscanf(fp1,"%d",&row1);
fscanf(fp2,"%d",&row2);

remcomment(&fp1);
remcomment(&fp2);

fscanf(fp1,"%d",&col1);
fscanf(fp2,"%d",&col2);

remcomment(&fp1);
remcomment(&fp2);

fscanf(fp1,"%d",&maxval1);
fscanf(fp2,"%d",&maxval2);

if( (strcmp(MagicChar1,"P5")) || (strcmp(MagicChar1,"P5")) )
{
  printf("\nInput Image in not in PGM Format !!\n");
  exit(1);
}

if( (strcmp(MagicChar1,MagicChar2)) || (row1 != row2)
        || (col1 != col2) || (maxval1 != maxval2) )
{
  printf("The two image are not of the same type !!\n");
```

```
    printf("Aborting ........\n");
    exit(1);
  }

  printf("\n\tMagic char = %s , row= %d ,col=%d
                ,maxval=%d\n\n",MagicChar1,row1,col1,maxval1);
  //Reading image into pixel
  for(i=0;i<row1;i++)
    for(j=0;j<col1;j++)
    {
      fscanf(fp1,"%c",&tmp1);
      fscanf(fp2,"%c",&tmp2);

      a[i][j]=(unsigned char)tmp1;
      b[i][j]=(unsigned char)tmp2;

    }

  fclose(fp1);
  fclose(fp2);

  //absolute percentage error
  APE();

  //error image
  error_image();

  return 0;

}

//for removing comment in PGM file
void remcomment(FILE **fp)
{
        char ch,buff[100];
        while(1)
        {
                ch=fgetc(*fp);
                while(WS(ch))
                        ch=fgetc(*fp);
                if(ch=='#')
                        fgets(buff,100,*fp);
                else break;
        }
        ungetc(ch,*fp);
```

```
}

void APE()
{
  int i,j,k;
  int diff,act;
  float err;

  diff=0;
  act=0;
  for(i=0;i<row1;i++)
    for(j=0;j<col1;j++){
      diff += (a[i][j]-b[i][j])*(a[i][j]-b[i][j]);
      act +=a[i][j]*a[i][j];
      //printf("diff=%d \t  act=%d\t",diff,act);
      //printf("a=%d , b=%d\n",a[i][j],b[i][j]);
    }

  err=sqrtf((float)diff)*100/sqrtf((float)act);

  printf("\n\tError :%f\n",err);

}

void error_image()
{
  int i,j,k;
  int zero=0,tmp;
  FILE *outfp;

  outfp=fopen("error_image.pgm","w");

  fprintf(outfp,"%s %d %d %d\n","P5",row1,col1,maxval1);

  for(i=0;i<row1;i++)
    for(j=0;j<col1;j++)
    {
      tmp=a[i][j]-b[i][j];
      //printf("%d \n",abs(tmp));
      fprintf(outfp,"%c",((abs(tmp) <=epsln )?  maxval1 : 0 ));
    }

  fclose(outfp);

}
```

References

1. J. Haselgrove and M. Prammer, An algorithm for compensating of surface-coil images for sensitivity of the surface coil, Magn. Reson. Imag., vol. 4, pp. 469-472, 1986.

2. E. R. McVeigh, M. J. Bronskill, and R. M. Henkelman, Phase and sensitivity of receiver coils in magnetic resonance imaging, Med. Phys., vol. 13, pp. 806-814, 1986.

3. A. Simmons, P. S. Tofts, G. J. Barker, and S. R. Arridge, Sources of intensity nonuniformity in spin echo images at 1.5 T, Magn. Reson. Med., vol. 32, pp. 121-128, 1994.

4. Z.-P. Liang and P. C. Lauterbur, Principles of Magnetic Resonance Imaging: A Signal Processing Perspective. Piscataway, NJ: IEEE Press, 1999.

5. M. D. Keiper, R. I. Grossman, J. A. Hirsch, L. Bolinger, I. L. Ott, L. J. Mannon, C. P. Langlotz, and D. L. Kolson, MR identification of white matter abnormalities in multiple sclerosis: A comparison between 1.5 T and 4 T, AJNR Amer. J. Neuroradiol., vol. 19, pp. 1489-1493, 1998.

6. M. Alecci, C. M. Collins, M. B. Smith, and P. Jezzard, Radio frequency magnetic field mapping of a 3 Tesla birdcage coil: Experimental and theoretical dependence on sample properties, Magn. Reson. Med., vol. 46, pp. 379-385, 2001.

7. Z. Chen, S. S. Li, J. Yang, D. Letizia, and J. Shen, Measurement and automatic correction of high-order B0 inhomogeneity in the rat brain at 11.7 Tesla, Magn. Reson. Imag., vol. 22, pp. 835-842, 2004.

8. L. Axel, J. Costantini, and J. Listerud, Intensity correction in surfacecoil MR imaging, AJR Amer. J. Roentgenol., vol. 148, pp. 418-420, 1987.

9. B. R. Condon, J. Patterson, D. Wyper, A. Jenkins, and D. M. Hadley, Image non-uniformity in magnetic resonance imaging: Its magnitude and methods for its correction, Br. J. Radiol., vol. 60, pp. 83-87, 1987.

10. D. A. Wicks, G. J. Barker, and P. S. Tofts, Correction of intensity nonuniformity in MR images of any orientation, Magn. Reson. Imag., vol. 11, pp. 183-196, 1993.

11. J. G. Sled and G. B. Pike, Standing-wave and RF penetration artifacts caused by elliptic geometry: An electrodynamic analysis of MRI, IEEE Trans. Med Imag., vol. 17, no. 4, pp. 653-662, Aug. 1998.

12. R. P. Velthuizen, J. J. Heine, A. B. Cantor, H. Lin, L. M. Fletcher, and L. P. Clarke, Review and evaluation of MRI nonuniformity corrections for brain tumor response measurements, Med. Phys., vol. 25, pp. 1655-1666, 1998.

13. J. B. Arnold, J. S. Liow, K. A. Schaper, J. J. Stern, J. G. Sled, D. W. Shattuck, A. J. Worth, M. S. Cohen, R. M. Leahy, J. C. Mazziotta, and D. A. Rottenberg, Qualitative and quantitative evaluation of six algorithms for correcting intensity nonuniformity effects, Neuroimage, vol. 13, pp. 931-943, 2001.

14. B. Belaroussi, J. Milles, S. Carme, Y. M. Zhu, and H. Benoit-Cattin, Intensity non-uniformity correction in MRI: Existing methods and their validation, Med. Image Anal., vol. 10, pp. 234-246, 2006.

15. J. G. Sled, A. P. Zijdenbos, and A. C. Evans, A nonparametric method for automatic correction of intensity nonuniformity in MRI data, IEEE Trans. Med. Imag., vol. 17, no. 1, pp. 87-97, Feb. 1998.

16. S. Prima, N. Ayache, T. Barrick, and N. Roberts, Maximum likelihood estimation of the bias field in MR brain images: Investigating different modelings of the imaging process, in Proc. Med. Image Comput. Computer-Assist. InterventionMICCAI 2001: 4th Int. Conf., Utrecht, The Netherlands, 2001, vol. 2208, pp. 811-819.

17. J. Sijbers, A. J. den Dekker, P. Scheunders, and D. Van Dyck, Maximum-likelihood estimation of Rician distribution parameters, IEEE Trans. Med Imag., vol. 17, no. 3, pp. 357-361, Jun. 1998.

18. C. Brechbhler, G. Gerig, and G. Szkely, Compensation of spatial inhomogeneity in MRI based on a multi-valued image model and a parametric bias estimate, in Proc. VBC 96 Visualization Biomed. Comput., New York, 1996, pp. 141146.

19. M. Styner, C. Brechbuhler, G. Szekely, and G. Gerig, Parametric estimate of intensity inhomogeneities applied to MRI, IEEE Trans. Med. Imag., vol. 19, no. 3, pp. 153-165, Mar. 2000.

20. D. L. Pham and J. L. Prince, Adaptive fuzzy segmentation of magnetic resonance images, IEEE Trans. Med. Imag., vol. 18, no. 9, pp. 737-752, Sep. 1999.

21. D. W. Shattuck, S. R. Sandor-Leahy, K. A. Schaper, D. A. Rottenberg, and R. M. Leahy, Magnetic resonance image tissue classification using a partial volume model, Neuroimage, vol. 13, pp. 856-876, 2001.

22. J. Ashburner and K. J. Friston, Unified segmentation, Neuroimage, vol. 26, pp. 839-851, 2005.

23. R. Guillemaud and M. Brady, Estimating the bias field ofMRimages, IEEE Trans. Med Imag., vol. 16, no. 3, pp. 238-251, Jun. 1997.

24. K. Van Leemput, F. Maes, D. Vandermeulen, and P. Suetens, Automated model-based bias field correction of MR images of the brain, IEEE Trans. Med. Imag., vol. 18, no. 10, pp. 885-896, Oct. 1999.

25. W. M.Wells, III, W. E. L. Grimson, R. Kikins, and F. A. Jolezs, Adaptive segmentation of MRI data, IEEE Trans. Med. Imag., vol. 15, no. 8, pp. 429-442, Aug. 1996.

26. B. Likar, M. A. Viergever, and F. Pernus, Retrospective correction of MR intensity inhomogeneity by information minimization, IEEE Trans. Med. Imag., vol. 20, no. 12, pp. 1398-1410, Dec. 2001.

27. B. Likar, J. B. Maintz, M. A. Viergever, and F. Pernus, Retrospective shading correction based on entropy minimization, J. Microsc., vol. 197, pt. 3, pp. 285-295, 2000.

28. J.-F. Mangin, Entropy minimization for automatic correction of intensity nonuniformity, presented at the IEEE Workshop Math. Methods Biomed. Image Anal. , Hilton Head Island, SC, 2000.

29. G. Collewet, A. Davenel, C. Toussaint, and S. Akoka, Correction of intensity nonuniformity in spin-echo T(1)-weighted images, Magn. Reson. Imag., vol. 20, pp. 365-373, 2002.

30. J. D. Gispert, S. Reig, J. Pascau, J. J. Vaquero, P. Garcia-Barreno, and M. Desco, Method for bias field correction of brain T1-weighted magnetic resonance images minimizing segmentation error, Hum. Brain Mapp., vol. 22, pp. 133-144, 2004.

31. M. Tincher, C. R. Meyer, R. Gupta, and D. M. Williams, Polynomial modeling and reduction of RF body coil spatial inhomogeneity in MRI, IEEE Trans. Med. Imag., vol. 12, no. 2, pp. 361-365, Jun. 1993.

32. W. W. Brey and P. A. Narayana, Correction for intensity falloff in surface coil magnetic resonance imaging, Med. Phys., vol. 15, pp. 241-245, 1988.

33. P. A. Narayana, W. W. Brey, M. V. Kulkarni, and C. L. Sievenpiper, Compensation for surface coil sensitivity variation in magnetic resonance imaging, Magn Reson Imag., vol. 6, pp. 271-274, 1988.

34. S. H. Lai and M. Fang, A dual image approach for bias field correction in magnetic resonance imaging, Magn. Reson. Imag., vol. 21, pp. 121-125, 2003.

35. A. Fan, W. M. Wells, J. W. Fisher, M. Cetin, S. Haker, R. Mulkern, C. Tempany, and A. S. Willsky, A unified variational approach to denoising and bias correction in MR, Inf. Process Med Imag., vol. 18, pp. 148-159, 2003.

36. H. Mihara, N. Iriguchi, and S. Ueno, A method of RF inhomogeneity correction in MR imaging, Magma, vol. 7, pp. 115-120, 1998.

37. K. P. Pruessmann, M. Weiger, M. B. Scheidegger, and P. Boesiger, SENSE: Sensitivity encoding for fast MRI, Magn. Reson. Med., vol. 42, pp. 952-962, 1999.

38. J. Y. Chiou, C. B. Ahn, L. T. Muftuler, and O. Nalcioglu, A simple simultaneous geometric and intensity correction method for echo-planar imaging by EPI-based phase modulation, IEEE Trans. Med Imag., vol. 22, no. 2, pp. 200-205, Feb. 2003.

39. D. L. Thomas, E. De Vita, R. Deichmann, R. Turner, and R. J. Ordidge, 3-D MDEFT imaging of the human brain at 4.7 T with reduced sensitivity to radiofrequency inhomogeneity, Magn. Reson. Med., vol. 53, pp. 1452-1458, 2005.

40. B. H. Brinkmann, A. Manduca, and R. A. Robb, Optimized homomorphic unsharp masking for MR grayscale inhomogeneity correction, IEEE Trans. Med. Imag., vol. 17, no. 2, pp. 161-171, Apr. 1998.

41. B. Johnston, M. S. Atkins, B. Mackiewich, and M. Anderson, Segmentation of multiple sclerosis lesions in intensity corrected multispectral MRI, IEEE Trans. Med. Imag., vol. 15, no. 2, pp. 154-169, Apr. 1996.

42. M. S. Cohen, R. M. DuBois, and M. M. Zeineh, Rapid and effective correction of RF inhomogeneity for high field magnetic resonance imaging, Hum. Brain Mapp., vol. 10, pp. 204-211, 2000.

43. L. Q. Zhou, Y. M. Zhu, C. Bergot, A. M. Laval-Jeantet, V. Bousson, J. D. Laredo, and M. Laval-Jeantet, A method of radio-frequency inhomogeneity correction for brain tissue segmentation in MRI, Comput. Med. Imag. Graph., vol. 25, pp. 379-389, 2001.

44. J. Russ, The Image Processing Handbook, 2nd ed. Piscataway, NJ: IEEE Press, 1995.

45. D. Tomazevic, B. Likar, and F. Pernus, Comparative evaluation of retrospective shading correction methods, J. Microsc., vol. 208, pp. 212-223, 2002.

46. E. B. Lewis and N. C. Fox, Correction of differential intensity inhomogeneity in longitudinal MR images, Neuroimage, vol. 23, pp. 75-83, 2004.

47. P. A. Narayana and A. Borthakur, Effect of radio frequency inhomogeneity correction on the reproducibility of intra-cranial volumes using MR image data, Magn. Reson. Med., vol. 33, pp. 396-400, 1994.

48. B. M. Dawant, A. P. Zijdenbos, and R. A. Margolin, Correction of intensity variations in MR images for computer-aided tissues classification, IEEE Trans. Med. Imag., vol. 12, no. 4, pp. 770-781, Dec. 1993.

49. Y. Zhuge, J. K. Udupa, J. Liu, P. K. Saha, and T. Iwanage, Scalebased method for correcting background intensity variation in acquired images, in Proc. SPIE Med. Imag. 2002: Image Process., 2002, vol. 4686, pp. 1103-1111.

50. P. Vemuri, E. G. Kholmovski, D. L. Parker, and B. E. Chapman, Coil sensitivity estimation for optimal SNR reconstruction and intensity inhomogeneity correction in phased array MR imaging, presented at the Inf. Process. Med. Imag.: 19th Int. Conf. (IPMI 2005), Glenwood Springs, CO, 2005.

51. J. A. Hernandez, M. L. Mora, E. Schiavi, and P. Toharia, RF inhomogeneity correction algorithm in magnetic resonance imaging, presented at the 5th Int. Symp. Biol. Medical Data Anal. (ISBMDA 2004), Barcelona, Spain, 2004.

52. J. Milles, Y. M. Zhu, N. Chen, L. P. Panych, G. Gimenez, and C. R. Guttmann, MRI intensity nonuniformity correction using simultaneously spatial and gray-level histogram information, in Proc. SPIE Med. Imag. 2004: Physiol., Function, Structure Med. Images, 2004, vol. 5370, pp. 734-742.

53. C. R. Meyer, P. H. Bland, and J. Pipe, Retrospective correction of intensity inhomogeneities in MRI, IEEE Trans. Med. Imag., vol. 14, no. 1, pp. 36-41, Mar. 1995.

54. S. H. Lai and M. Fang, A new variational shape-from-orientation approach to correcting intensity inhomogeneities in magnetic resonance images, Med. Image Anal., vol. 3, pp. 409-424, 1999.

55. A. Koivula, J. Alakuijala, and O. Tervonen, Image feature based automatic correction of low-frequency spatial intensity variations in MR images, Magn. Reson. Imag., vol. 15, pp. 1167-1175, 1997.

56. E. A. Vokurka, N. A. Thacker, and A. Jackson, A fast model independent method for automatic correction of intensity nonuniformity in MRI data, J. Magn. Reson. Imag., vol. 10, pp. 550-562, 1999.

57. E. A. Vokurka, N. A. Watson, Y. Watson, N. A. Thacker, and A. Jackson, Improved high resolution MR imaging for surface coils using automated intensity non-uniformity correction: Feasibility study in the orbit, J. Magn. Reson. Imag., vol. 14, pp. 540-546, 2001.

58. A. H. Andersen, Z. Zhang, M. J. Avison, and D. M. Gash, Automated segmentation of multispectral brain MR images, J. Neurosci. Meth., vol. 122, pp. 13-23, 2002.

59. X. Li, L. Li, H. Lu, and Z. Liang, Partial volume segmentation of brain magnetic resonance images based on maximum a posteriori probability, Med. Phys., vol. 32, pp. 2337-2345, 2005.

60. K. Van Leemput, F. Maes, D. Vandermeulen, A. Colchester, and P. Suetens, Automated segmentation of multiple sclerosis lesions by model outlier detection, IEEE Trans. Med Imag., vol. 20, no. 8, pp. 677-688, Aug. 2001.

61. J. D. Gispert, S. Reig, J. Pascau, R. M. Lazaro, J. J. Vaquero, and M. Desco, Inhomogeneity correction of magnetic resonance images by minimization of intensity overlapping, presented at the 2003 Int. Conf. Image Process. (ICIP 2003), Barcelona, Catalonia, Spain, 2003.

62. R. Bansal, L. H. Staib, and B. S. Peterson, Correcting nonuniformities in MRI intensities using entropy minimization based on an elastic model, presented at the Medical Image Computing and Computer-Assisted Intervention (MICCAI 2004), Saint-Malo, France, 2004.

63. J. C. Rajapakse and F. Kruggel, Segmentation of MR images with intensity inhomogeneities, Image And Vision Comput., vol. 16, pp. 165-180, 1998.

64. S.-G. Kim, S.-K. Ng, G. J. McLachlan, and W. Deming, Segmentation of brain MR images with bias field correction, presented at the APRS Workshop Digital Image Computing: WDIC 2003, St. Lucia, Brisbane, Australia, 2003.

65. G. Gerig, M. Prastawa, W. Lin, and J. Gilmore, Assessing early brain development in neonates by segmentation of high-resolution 3T MRI, presented at the 6th Int. Conf. Medical Image Comput. Computer-Assisted Intervention (MICCAI 2003), , Montreal, ON, Canada, 2003.

66. J. C. Rajapakse, J. N. Giedd, and J. L. Rapoport, Statistical approach to segmentation of single-channel cerebral MR images, IEEE Trans. Med. Imag., vol. 16, no. 2, pp. 176-186, Apr. 1997.

67. Y. Zhang, M. Brady, and S. Smith, Segmentation of brain MR images through a hidden Markov random field model and the expectation- maximization algorithm, IEEE Trans. Med Imaging, vol. 20, no. 1, pp. 45-57, Jan. 2001.

68. K. Van Leemput, F. Maes, D. Vandermeulen, and P. Suetens, Automated model-based tissue classification of MR images of the brain, IEEE Trans. Med. Imag., vol. 18, no. 10, pp. 897908, Oct. 1999.

69. J. C. Bezdek, L. O. Hall, and L. P. Clarke, Review of MR image segmentation techniques using pattern recognition, Med. Phys., vol. 20, pp. 1033-1048, 1993.

70. D. L. Pham and J. L. Prince, An adaptive fuzzy C-means algorithm for the image segmentation in the presence of intensity inhomogeneities, Pattern Recognit. Lett., vol. 20, pp. 57-68, 1998.

71. M. N. Ahmed, S. M. Yamany, A. A. Farag, and T. Moriarty, Bias field estimation and adaptive segmentation of MRI data using amodified fuzzy C-means algorithm, presented at the IEEE Int. Conf. Comput. Vision Pattern Recognit. (CVPR99), Fort Collins, CO, 1999.

72. M. N. Ahmed, S. M. Yamany, N. Mohamed, A. A. Farag, and T. Moriarty, A modified fuzzy C-means algorithm for bias field estimation and segmentation of MRI data, IEEE Trans. Med. Imag., vol. 21, no. 3, pp. 193-199, Mar. 2002.

73. A. W. Liewand H.Yan, An adaptive spatial fuzzy clustering algorithm for 3-DMRimage segmentation, IEEE Trans. Med. Imag., vol. 22, no. 9, pp. 1063-1075, Sep. 2003.

74. C. Zhu and T. Jiang, Multicontext fuzzy clustering for separation of brain tissues in magnetic resonance images, Neuroimage, vol. 18, pp. 685-696, 2003.

75. B. Likar, J. Derganc, and F. Pernus, Segmentation-based retrospective correction of intensity non-uniformity in multi-spectralMRimages, in Proc. SPIE Med. Imag. 2002: Image Process., San Diego, 2002, vol. 4684, pp. 1531-1540.

76. J. Derganc, B. Likar, and F. Pernus, Nonparametric segmentation of multispectral MR images incorporating spatial and intensity information, in Proc. SPIE Med. Imag. 2002: Image Process., San Diego, CA, 2002, vol. 4684, pp. 391-400.

77. P. A. Viola, Alignment by maximization of mutual information, Ph.D. dissertation, Mass. Inst. Technol., Cambridge, 1995.

78. B. Likar, M. A. Viergever, and F. Pernus, Retrospective correction of mr intensity inhomogeneity by information minimization, presented at the 3rd Int. Conf. Med. Image Comput. Computer-Assisted Intervention (MICCAI 2000), Pittsburgh, PA, 2000.

79. E. Solanas and J.-P. Thiran, Exploiting voxel correlation for automated MRI bias field correction by conditional entropy minimization, presented at the 4th Int. Medical Image Comput. Computer-Assist. Intervent. (MICCAI 2001), Utrecht, The Netherlands, 2001.

80. E. G. Learned-Miller and P. Ahammad, Joint MRI bias removal using entropy minimization across images, presented at the Neural Inf. Proces. Syst. Conf. (NIPS), Vancouver, Canada, 2004.

81. U. Vovk, F. Pernus, and B. Likar, MRI intensity inhomogeneity correction by combining intensity and spatial information, Phys. Med. Biol., vol. 49, pp. 4119-4133, 2004.

82. , Intensity inhomogeneity correction of multispectral MR images, Neuroimage, vol. 32, pp. 54-61, 2006.

83. C. Studholme, V. Cardenas, E. Song, F. Ezekiel, A. Maudsley, and M. Weiner, Accurate template-based correction of brain MRI intensity distortion with application to dementia and aging, IEEE Trans. Med Imag., vol. 23, no. 1, pp. 99-110, Jan. 2004.

84. J. Luo, Y. Zhu, P. Clarysse, and I. Magnin, Correction of bias field in MR images using singularity function analysis, IEEE Trans. Med. Imag., vol. 24, no. 8, pp. 1067-1085, Aug. 2005.

85. B. Fischl, D. H. Salat, A. J. van der Kouwe, N. Makris, F. Segonne, B. T. Quinn, and A. M. Dale, Sequence-independent segmentation of magnetic resonance images, Neuroimage, vol. 23, no. Suppl 1, pp. S69-S84, 2004.

86. R. C. Jain, T. O. Binford, M. A. Snyder, Y. Aloimonos, A. Rosenfeld, T. S. Huang, K. W. Bowyer, and J. P. Jones, Ignorance, myopia, and naivete in computer vision systems, Comput. Vision, Graphics, Image Process. : Image Understanding, vol. 53, pp. 112-117, 1991.

87. A. Montillo, J. K. Udupa, L. Axel, and D. N. Metaxas, Interaction between noise suppression and inhomogeneity correction in MRI, in Proc. SPIE Med. Imag. 2003: Image Process., 2003, vol. 5032, pp. 1025-1036.

88. M. X. H. Yan and J. S. Karp, An adaptive Bayesian approach to threedimensionalMRbrain segmentation, in Proc. Inf. Process. Med. Imag. (IPMI95), 1995, vol. 20, pp. 12-13.

89. J. Ashburner and K. J. Friston, Voxel-based morphometrythe methods, Neuroimage, vol. 11, pp. 805-821, 2000.

90. C. A. Cocosco, V. Kollokian, K. R. K. -S. Kwan, and A. C. Evans, BrainWeb: Online interface to a 3-D MRI simulated brain database, NeuroImage, vol. 5, pp. 425-425, 1997.

91. D. L. Collins, A. P. Zijdenbos, V. Kollokian, J. G. Sled, N. J. Kabani, C. J. Holmes, and A. C. Evans, Design and construction of a realistic digital brain phantom, IEEE Trans. Med Imag., vol. 17, no. 3, pp. 463-468, Jun. 1998.

92. H. Benoit-Cattin, G. Collewet, B. Belaroussi, H. Saint-Jalmes, and C. Odet, The SIMRI project: A versatile and interactive MRI simulator, J. Magn. Reson., vol. 173, pp. 97-115, 2005.

93. T. S. Ibrahim, C. Mitchell, P. Schmalbrock, R. Lee, and D. W. Chakeres, Electromagnetic perspective on the operation of RF coils at 1.511.7 Tesla, Magn. Reson. Med., vol. 54, pp. 683-690, 2005.

94. T. S. Ibrahim, A. Kangarlu, and D. W. Chakeress, Design and performance issues of RF coils utilized in ultra high field MRI: Experimental and numerical evaluations, IEEE Trans. Biomed. Eng., vol. 52, no. 7, pp. 1278-1284, Jul. 2005.

95. H. Uematsu, L. Dougherty, M. Takahashi, Y. Ohno, M. Nakatsu, M. D. Schnall, and H. Hatabu, Abdominal imaging at 4 T MR system: A preliminary result, Eur. J. Radiol., vol. 47, pp. 161-163, 2003.